ATHEROSCLEROSIS

Targeting a cell-specific microRNA repressor of CXCR4 ameliorates atherosclerosis in mice

Ismail Cimen[1]†‡, Lucia Natarelli[1]‡, Zahra Abedi Kichi[1], James M. Henderson[1,2], Floriana M. Farina[1,2], Eva Briem[3], Maria Aslani[1]§, Remco T.A. Megens[1,2,4], Yvonne Jansen[1], Elizabeth Mann-Fallenbuchel[1], Selin Gencer[1]†, Johan Duchêne[1,2], Maliheh Nazari-Jahantigh[1,2], Emiel P.C. van der Vorst[1,2,5,6], Wolfgang Enard[3], Yvonne Döring[1,2,7], Andreas Schober[1,2], Donato Santovito[1,2,8]*||, Christian Weber[1,2,9,10]*||

The CXC chemokine receptor 4 (CXCR4) in endothelial cells (ECs) and vascular smooth muscle cells (VSMCs) is crucial for vascular integrity. The atheroprotective functions of CXCR4 in vascular cells may be counteracted by atherogenic functions in other nonvascular cell types. Thus, strategies for cell-specifically augmenting CXCR4 function in vascular cells are crucial if this receptor is to be useful as a therapeutic target in treating atherosclerosis and other vascular disorders. Here, we identified miR-206-3p as a vascular-specific CXCR4 repressor and exploited a target-site blocker (CXCR4-TSB) that disrupted the interaction of miR-206-3p with CXCR4 in vitro and in vivo. In vitro, CXCR4-TSB enhanced CXCR4 expression in human and murine ECs and VSMCs to modulate cell viability, proliferation, and migration. Systemic administration of CXCR4-TSB in *Apoe*-deficient mice enhanced *Cxcr4* expression in ECs and VSMCs in the walls of blood vessels, reduced vascular permeability and monocyte adhesion to endothelium, and attenuated the development of diet-induced atherosclerosis. CXCR4-TSB also increased CXCR4 expression in B cells, corroborating its atheroprotective role in this cell type. Analyses of human atherosclerotic plaque specimens revealed a decrease in CXCR4 and an increase in miR-206-3p expression in advanced compared with early lesions, supporting a role for the miR-206-3p–CXCR4 interaction in human disease. Disrupting the miR-206-3p–CXCR4 interaction in a cell-specific manner with target-site blockers is a potential therapeutic approach that could be used to treat atherosclerosis and other vascular diseases.

INTRODUCTION

Atherosclerosis is a chronic inflammatory disease of the arterial wall and the pathophysiological substrate of acute coronary syndromes and ischemic strokes (*1*), which are the major causes of mortality and disability worldwide (*2*, *3*). Despite the substantial improvement in clinical management (*4*), the incidence and prevalence of cardiovascular disease increased over the past 30 years with a high mortality burden (*2*), mandating a quest to identify additional targets to reduce the residual risk of cardiovascular events. Lipid-lowering approaches are the cornerstone of preventive cardiology, but other molecular mechanisms, for instance, by driving inflammation and (auto-)immune responses, are currently being explored for therapeutic purposes (*5*, *6*). Yet approaches more generally targeting inflammatory mediators and pathways (such as canakinumab and colchicine) were accompanied by side effects in clinical trials (*5*, *6*), and the identification of previously unidentified targets for tailored enhancement of vascular health remains an unmet clinical need in cardiovascular medicine.

Chemokines and their receptors have been implicated as players and possible therapeutic targets in atherosclerosis (*1*, *5*, *6*). Beyond its role in leukocyte trafficking, the chemokine receptor CXCR4 is essential for embryonic angiogenesis and vessel integrity in adulthood (*7*, *8*). In mice, conditional deletion of *Cxcr4* in endothelial cells (ECs) or vascular smooth muscle cells (VSMCs) aggravates atherosclerosis by disrupting endothelial integrity and promoting VSMC dedifferentiation, respectively (*8*). Consistently, the genetic variant rs2322864 is associated with lower *CXCR4* expression in atherosclerotic plaques and a higher prevalence of coronary heart disease in humans (*8*), and another variant (namely, rs4954580) in the *CXCR4* locus also showed a significant ($P = 3.0 \times 10^{-9}$) association (*9*). This evidence from human and mouse studies unveils the therapeutic opportunity of selectively enhancing the CXCR4 pathway. Yet *CXCR4* is ubiquitously expressed, and mice with inducible global deletion of *Cxcr4* failed to replicate the atheroprone phenotype of EC- or VSMC-specific deficiency (*8*). Although CXCR4 antagonists and conditional deletion of *Cxcr4* revealed the protective role of CXCR4 in neutrophils and B cells (*10*–*12*), atherogenic properties of CXCR4 in other cell types [for instance,

[1]Institute for Cardiovascular Prevention (IPEK), Ludwig-Maximilians-Universität München, 80336 Munich, Germany. [2]German Centre for Cardiovascular Research (DZHK), partner site Munich Heart Alliance, 80336 Munich, Germany. [3]Anthropology and Human Genomics, Faculty of Biology, Ludwig-Maximilians-Universität München, 85152 Planegg-Martinsried, Germany. [4]Department of Biomedical Engineering, Cardiovascular Research Institute Maastricht (CARIM), Maastricht University Medical Centre, 6200 MD Maastricht, Netherlands. [5]Institute for Molecular Cardiovascular Research (IMCAR), RWTH Aachen University, 52074 Aachen, Germany. [6]Interdisciplinary Center for Clinical Research (IZKF), RWTH Aachen University, 52062 Aachen, Germany. [7]Department of Angiology, Swiss Cardiovascular Center, Inselspital, University Hospital of Bern, 3010 Bern, Switzerland. [8]Institute of Genetic and Biomedical Research (IRGB), Unit of Milan, National Research Council (CNR), 20090 Milan, Italy. [9]Department of Biochemistry, Cardiovascular Research Institute Maastricht (CARIM), Maastricht University Medical Centre, 6229 HX Maastricht, Netherlands. [10]Munich Cluster for Systems Neurology (SyNergy), 81337 Munich, Germany.
*Corresponding author. Email: chweber@med.lmu.de (C.W.); donato.santovito@med.uni-muenchen.de (D.S.)
†Present address: Bay Area Institute of Science, Altos Labs, 2200 Bridge Parkway, Redwood City, CA 94065, USA.
‡These authors contributed equally to this work.
§Present address: Institute for Bioinnovation, Biomedical Sciences Research Center Alexander Fleming, 16672 Vari, Greece.
||These authors contributed equally to this work.

progenitor cells; (*13*)] are likely to occur. Hence, the development of strategies selectively boosting CXCR4 in vascular cells is crucial for targeting this receptor for therapeutic purposes.

The gene expression landscape of every cell type undergoes multiple layers of regulation, ranging from cell-specific enhancers controlling chromatin accessibility to posttranscriptional mechanisms (*14*–*16*). The latter include microRNAs (miRNAs), small noncoding RNAs that bind complementary sequences [termed miRNA-responsive elements (MREs)] of target RNA transcripts (*15*) to guide their decay or translational repression within the RNA-induced silencing complex (RISC) (*15*, *16*). As a class, miRNAs are crucially involved in atherosclerosis, and their modulation (by inhibitors or mimics) represents an attractive therapeutic option (*16*, *17*). The transcription of miRNA precursors is cell specific and minimally influenced by exogenous stimuli, including proatherogenic ones (*18*). This translates into a cell-specific pattern of miRNA expression, as exemplified in the vessel wall by miR-126 in ECs or miR-143/145 in VSMCs, both involved in atherogenesis (*18*–*22*). Previous studies have shown how miRNAs regulate CXCR4 in diverse cell types, as in the case of miR-146a-5p in megakaryocyte progenitors or miR-139-5p in ECs (*23*, *24*). Thus, we hypothesized that miRNAs specifically restricted to vascular cells (namely, ECs and VSMCs) are involved in a network for cell-specific regulation of CXCR4 that could be targeted by antisense oligonucleotides disrupting the miRNA–target RNA interaction.

RESULTS

CXCR4 is specifically targeted by miR-206-3p in vascular cells

To explore the overall contribution of miRNAs in the regulation of CXCR4 in the aortic wall, we retrieved data on *Cxcr4* expression from available transcriptomic datasets of aortas of mice with cell-specific *Dicer1* deletion in ECs ($Apoe^{-/-}Cdh5\text{-}CreER^{T2}Dicer1^{fl/fl}$) or VSMCs ($Apoe^{-/-}Smmhc\text{-}iCreER^{T2}\ Dicer1^{fl/fl}$) (*25*–*28*). Higher expression of *Cxcr4* (but not of its ligand *Cxcl12* and the alternative receptor *Ackr3*) was found in both models, reaching statistical significance for *Dicer1* depletion in VSMCs ($P = 1.9 \times 10^{-3}$). In contrast, *Cxcr4* was significantly down-regulated ($P = 5.6 \times 10^{-20}$) upon deletion of *Dicer1* in macrophages derived from monocytes of $Apoe^{-/-}LysM\text{-}CreDicer1^{fl/fl}$ (Fig. 1A). These data were validated in loss-of-function experiments in vitro. Silencing of *Dicer1* was effectively obtained by transfecting GapmeRs in murine aortic ECs (MAoECs) and aortic VSMCs (MOVAS), as confirmed by quantitative polymerase chain reaction (qPCR) (fig. S1A), and was associated with an increase in CXCR4 mRNA and protein, as assessed by qPCR and Western blot (Fig. 1, B and C). We also sought to explore whether the miRNA-dependent regulatory mechanism is conserved in humans. To this end, we performed loss-of-function experiments in human aortic ECs (HAoECs), VSMCs (HAoSMCs), and macrophages [THP-1 cells stimulated with phorbol 12-myristate 13-acetate (PMA)] (fig. S1A). We detected an increase in CXCR4 at the protein level upon *DICER1* knockdown in HAoECs and HAoSMCs by immunoblotting (Fig. 1D). Conversely, deletion of *DICER1* in THP-1–derived macrophages did not influence the expression of CXCR4 (Fig. 1D). Together, these findings uncover a miRNA-mediated repressive pathway for CXCR4 in ECs and VSMCs of murine aortas but not in myeloid cells, which can also be observed for CXCR4 protein in human primary cells and likely in human arteries.

Having established the net contribution of miRNAs as a class, we next aimed to identify specific miRNA(s) responsible for regulating CXCR4 in ECs and VSMCs. We applied a multistep screening approach (Fig. 1E and table S1): First, we referred to TargetScan (v8.0) for miRNAs with predicted binding sites in the 3′ untranslated region (3′UTR) of the *CXCR4* transcript to identify 188 and 193 miRNAs in humans and mice, respectively. We then restricted our analyses to 10 miRNAs pairing to binding sites with high evolutionary conservation (branch length score ≥ 2.0 for 8-mer or ≥ 3.0 for 7-mer-m8 MREs). Among those, we focused on a set of six miRNAs, which belong to families broadly conserved in metazoans in the evolutionary data of MirGeneDB (v2.0) (*29*, *30*). Aiming for a possible role in vascular biology, we interrogated the CAGE (cap analysis of gene expression) datasets of the FANTOM5 project (*31*, *32*) to find that only three of these miRNAs (miR-140-3p, miR-1-3p, and miR-206-3p) were detectable in murine adult aortas (ID# FF46-23H1). With the major purpose of identifying miRNAs expressed in ECs and VSMCs but not in macrophages, we excluded miR-140-3p, because its expression was detected in the CAGE datasets of murine macrophages (ID# FF2171-50H8, FF3704-170A1, FF3632-171A1, and FF3704-172A1). Conversely, miR-1-3p and miR-206-3p, members of the same miRNA family, were not retrieved in this dataset, indicating an exclusive expression in vascular cells but not macrophages. We experimentally validated the ability of these miRNAs to repress *Cxcr4* in a reporter assay detecting reduced luciferase activity in human embryonic kidney (HEK) 293 cells transfected with mimics of miR-1-3p or miR-206-3p but not with scrambled mimics or empty vectors (Fig. 1F). Using the same assay, we also tested 19 additional miRNAs predicted to target *Cxcr4* and expressed in macrophages (selected from literature and expression datasets), and although a slight effect was observed for miR-132-3p, none of these miRNAs caused a substantial reduction in luciferase activity (fig. S1, B and C). These findings imply that macrophage miRNAs are insufficient in repressing CXCR4 and may thus explain the discrepancy in the regulatory role of DICER1 between vascular cells and macrophages (Fig. 1, C and D). Together, we identified a miRNA family (miR-1/miR-206), conserved in metazoans (fig. S1D), as a putative regulator of CXCR4 in vascular cells.

Among the members of the miR-1/miR-206 family, miR-1-3p is enriched in the heart and contributes to cardiac homeostasis and function (*33*–*35*). For this reason, we decided to investigate miR-206-3p to minimize the risk of possible off-target gene regulation in cardiomyocytes. To validate miR-206-3p as a vascular cell–specific modulator of CXCR4, we first measured the expression of this miRNA by qPCR in MAoECs, MOVAS, and bone marrow–derived macrophages (BMDMs). The expression of miR-206-3p was detected at the highest amount in MAoECs, was slightly lower in MOVAS, and was negligible in BMDMs (Fig. 1G). To prove a regulatory role, we performed gain- and loss-of-function experiments by transfecting miR-206-3p mimics and inhibitors in MAoECs and MOVAS before assessing the CXCR4 expression at mRNA and protein levels by qPCR and Western blot, respectively. Transfection of mimics and inhibitors effectively modulated miR-206-3p expression (fig. S1, E and F). Consistent with a posttranscriptional repressive role of miR-206-3p, treatment with mimics reduced the expression of CXCR4 in both cell types (Fig. 1H). In contrast,

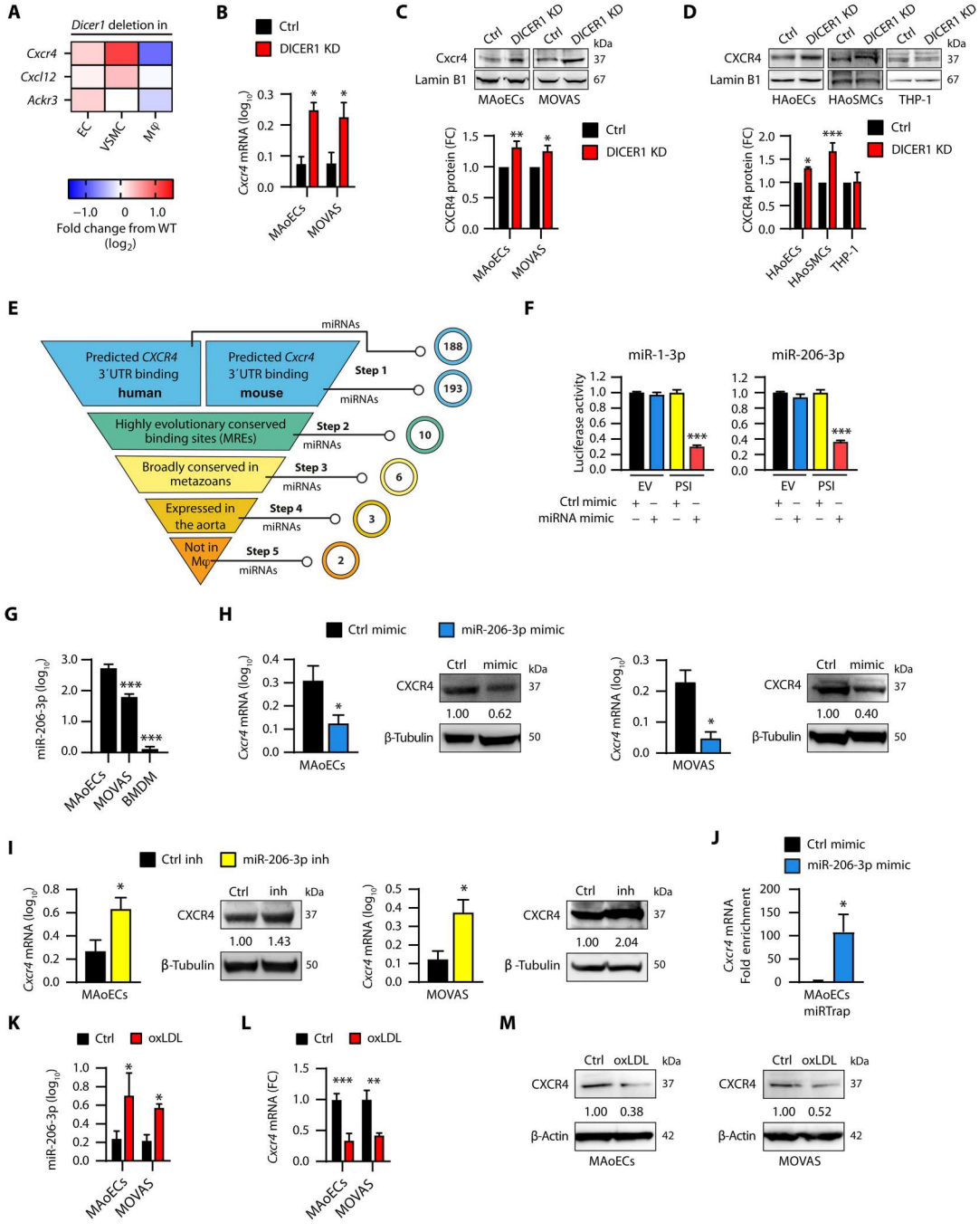

Fig. 1. Identification of miR-206-3p as a CXCR4 repressor in vascular cells. (**A**) *Cxcr4*, *Cxcl12*, and *Ackr3* expression from transcriptional datasets of mice with *Dicer1* deletion in ECs, VSMCs, or myeloid cells (Mϕ). (**B** and **C**) Expression of CXCR4 at the mRNA (B) and protein (C) levels in MAoECs and MOVAS without (Ctrl) and with GapmeR-mediated silencing of *Dicer1* (DICER1 KD), as assessed by qPCR or Western blot, respectively (n = 3 to 6). KD, knockdown. (**D**) Representative immunoblotting and quantification of CXCR4 expression at the protein level in HAoECs, HAoSMCs, and THP-1–derived macrophages without (Ctrl) and with silencing of *DICER1* (DICER1 KD) (n = 4). (**E**) Workflow for identifying the candidate miRNAs for repression of *CXCR4* in vascular cells (see the main text and table S1 for further details). (**F**) Dual-luciferase reporter assays were performed on HEK cells by cotransfection of miR-1-3p or miR-206-3p mimics with a luciferase reporter gene linked to the 3′UTR of *Cxcr4* (n = 5). (**G**) Quantification by qPCR of miR-206-3p expression in ECs, VSMCs, and BMDMs (n = 4 to 8). (**H** and **I**) Quantification of *Cxcr4* mRNA by qPCR and representative Western blot for CXCR4 protein in MAoECs and MOVAS transfected with miR-206-3p mimics (mimic) (H), LNA-antisense inhibitors (inh) (I), or scrambled oligonucleotides (Ctrl) (n = 3 or 4). Western blot panels representative of three replicates per group. (**J**) Fold enrichment of *Cxcr4* transcript in the RISC immunoprecipitated after transfection of MAoECs with miR-206-3p mimics together with the miRTrap vector expressing a modified GW182 protein trapping miRNA:mRNA complexes. Data are normalized to cells transfected with scrambled oligonucleotides (n = 4). (**K**) Expression of miR-206-3p in MAoECs and MOVAS treated with oxLDL (100 μg/ml) for 24 hours or controls (Ctrl) as assessed by qPCR (n = 7). (**L** and **M**) Quantification of *Cxcr4* mRNA by qPCR and representative Western blot for CXCR4 protein in MAoECs and MOVAS treated with oxLDL (100 μg/ml) for 24 hours or controls (Ctrl) (n = 6). Data are presented as means and SEM and analyzed by factorial (B to D and K and L) or univariate (F and G) ANOVA with Bonferroni post hoc test or by Student's t test (H to J). $^*P < 0.05$; $^{**}P < 0.01$; $^{***}P < 0.001$.

miR-206-3p inhibitors strongly increased CXCR4 expression (Fig. 1I), thus confirming the regulatory role of endogenous miR-206-3p in MAoECs and MOVAS. Moreover, we confirmed the RISC-loading of *Cxcr4* mRNA by immunoprecipitating the RISC in MAoECs cotransfected with miR-206-3p mimics and the pMir-Trap vector, which expresses a tagged C-terminal truncated GW182 protein to enable the capture of miRNA targets and their immunoprecipitation (Fig. 1J). Next, we exposed MAoECs and MOVAS to oxidized low-density lipoproteins (oxLDL, 100 μg/ml) for 24 hours to mimic an atherogenic environment in vitro. This treatment resulted in an increase in miR-206-3p (Fig. 1K) paralleled by lower expression of CXCR4 mRNA and protein compared with controls

(Fig. 1, L and M), thus demonstrating the relevance of this regulatory axis under atherogenic conditions. Last, consistent with the relevance of miR-206-3p as a vascular-specific *Cxcr4* regulator, an analysis of the publicly available transcriptional data [Gene Expression Omnibus (GEO) ID# GSE34054] revealed lower expression of miR-206-3p in carotid arteries of mice with genetic deletion of *Dicer1* in VSMCs (fig. S1G). This supports a vascular origin, and integrative target prediction analysis combining mRNA and miRNA transcriptomes using MAGIA[2] (miRNA and genes integrated analysis 2) (*36*) unveiled a significant interaction between miR-206-3p and *Cxcr4* mRNA ($q = 1.8 \times 10^{-3}$). Together, our results show that miR-206-3p is enriched in ECs and VSMCs and mediates a repressive pathway for CXCR4 by direct interaction with the 3′UTR of its transcript.

Disrupting the miR-206-3p–CXCR4 interaction affects EC and VSMC function in vitro

We showed the regulatory role of miR-206-3p on CXCR4 expression in vascular cells; however, 125 experimentally validated targets are reported for miR-206-3p in the latest release of miRTarbase (v8.0) (*37*). Hence, miR-206-3p inhibitors may be burdened by side effects from the derepression of transcripts other than CXCR4. To specifically modulate the miR-206-3p–CXCR4 interaction, we designed locked nucleic acid (LNA)–modified oligonucleotides [termed CXCR4–target site blocker (CXCR4-TSB)] pairing the MRE mapped to nucleotides 3545 to 3352 of human *CXCR4* transcript (and nucleotides 1448 to 1468 of the 3′UTR of murine *Cxcr4* mRNA) to prevent binding with miR-206-3p (Fig. 2A). Compared with cells treated with a scrambled LNA oligonucleotide, transfection of HAoECs and HAoSMCs with the CXCR4-TSB effectively increased the expression of CXCR4 mRNA and protein, as shown by qPCR and Western blotting (Fig. 2, B and C). To gain more comprehensive insights into the transcriptional effects and specificity of CXCR4-TSB, we further analyzed the transcriptome of oxLDL-exposed HAoECs treated with CXCR4-TSB or a scrambled oligonucleotide using an efficient bulk RNA-sequencing (RNA-seq) method (Prime-seq) (*38*). Higher expression of CXCR4 was also observed in the RNA-seq (fig. S2A). Yet none of the 17,256 detected genes showed a difference in mRNA expression despite considerable statistical power to detect them (*38*). In particular, no differences were evident in other validated targets of miR-206-3p (fig. S2B), as confirmed for *NOTCH3*, *VEGFA*, and *GJA1* by qPCR in HAoECs and HAoSMCs (Fig. 2, B and C). These findings indicate that CXCR4-TSB exerts biological functions in HAoECs by posttranscriptional mechanisms and rather subtle transcriptional changes (*39*). On the other hand, dimensional reduction of transcriptomic data by principal components analysis revealed a distinct transcriptional signature upon CXCR4-TSB treatment, which was not observed after CXCR4 silencing using short hairpin RNAs (shRNAs) (fig. S2, C and D), indicating that the subtle effects on the transcriptional profile may be related to *CXCR4*. The ability of CXCR4-TSB to increase CXCR4 expression without affecting other validated targets was also evident in MAoECs and MOVAS (Fig. 2, D and E). Cumulatively, our data establish that CXCR4-TSB treatment is an effective approach for selectively enhancing CXCR4 expression in vascular cells in humans and mice.

We previously reported CXCR4 deficiency to drive proatherogenic features in ECs (*8*). Thus, we investigated whether enhancing its expression by CXCR4-TSB promotes beneficial outcomes. Consistent with the relevance of the miR-206-3p–CXCR4 axis in atherogenic conditions (Fig. 1, K to M), not only did the CXCR4-TSB substantially increase CXCR4 expression in HAoECs grown under standard conditions, but this effect was also enhanced in cells exposed to oxLDL (Fig. 3, A and B). In line with the functional relevance of boosting CXCR4, we measured higher rates of proliferation by 5-ethynyl-2′-deoxyuridine (EdU)–incorporation assays (Fig. 3C) and higher migratory capacity in wound healing assays (Fig. 3D) using HAoECs transfected with CXCR4-TSB versus scrambled control. Moreover, CXCR4-TSB mitigated the increase in apoptosis (as assessed by a caspase-3/7 activity assay; Fig. 3E) and in permeability for fluorescently labeled dextran (Fig. 3F) triggered by oxLDL treatment. In addition, we found that treatment with CXCR4-TSB blunted the increase in monocyte adhesion to an endothelial monolayer activated by oxLDL (Fig. 3G). Identical outcomes were observed in MAoECs (fig. S3), confirming the conservation of this regulatory axis across species. Last, rescue experiments in HAoECs revealed that silencing of CXCR4 by shRNA prevented the CXCR4-TSB–induced enhancement of proliferation and migration both in the presence and in the absence of oxLDL (Fig. 3, H to J), validating the mechanistic requirement of CXCR4. Of note, silencing of CXCR4 also reduced proliferation and migration in control cells, supporting its relevance for EC homeostasis (Fig. 3, I and J). Together, these data provide functional evidence for the ability of CXCR4-TSB to promote endothelial integrity and antiatherogenic features in vitro.

Because the deletion of CXCR4 also affects the atherogenic functions of VSMCs (*8*), we next explored the effects of CXCR4-TSB on human and murine VSMCs. As observed in ECs, treatment with CXCR4-TSB enhanced the expression of CXCR4 mRNA and protein in HAoSMCs and MOVAS with or without oxLDL stimulation (Fig. 4, A and B; and fig. S4, A and B). In contrast to ECs, the CXCR4-TSB repressed the higher proliferative rate and migration capacity induced by treatment with oxLDL in HAoSMCs and MOVAS, as assessed by EdU incorporation and wound healing assays, respectively (Fig. 4, C and D, and fig. S4, C and D). This was consistent with the maintenance of a differentiated VSMC phenotype, because treatment with CXCR4-TSB prevented the oxLDL-mediated decrease in the contraction marker MYH11 (SMMHC) (Fig. 4, E and F, and fig. S4E). Whereas silencing of CXCR4 increased proliferation and migration in control HAoSMCs, CXCR4-TSB treatment did not reduce proliferation and migration after silencing of CXCR4 in HAoSMCs in the presence or absence of oxLDL (Fig. 4, G to I). These results show that CXCR4-TSB can increase CXCR4 expression to promote and sustain a quiescent phenotype of VSMCs.

CXCR4-TSB prevents hyperlipidemia-induced endothelial dysfunction in vivo

We next tested whether the antiatherogenic properties of CXCR4-TSB observed in vitro can be recapitulated in an atheroprone *Apoe*$^{-/-}$ mouse model of advanced atherosclerosis. Mice were fed a Western diet (WD) for 16 weeks and received weekly systemic administration of CXCR4-TSB or control scrambled LNA oligonucleotides (0.4 mg/20 g, intravenously) for the final 4 weeks (Fig. 5A). Immunofluorescence staining revealed increased expression of CXCR4 in atherosclerotic lesions of the aortic root upon treatment with CXCR4-TSB. Quantitative analysis of mean fluorescence intensity (MFI) revealed that treatment with CXCR4-TSB promoted

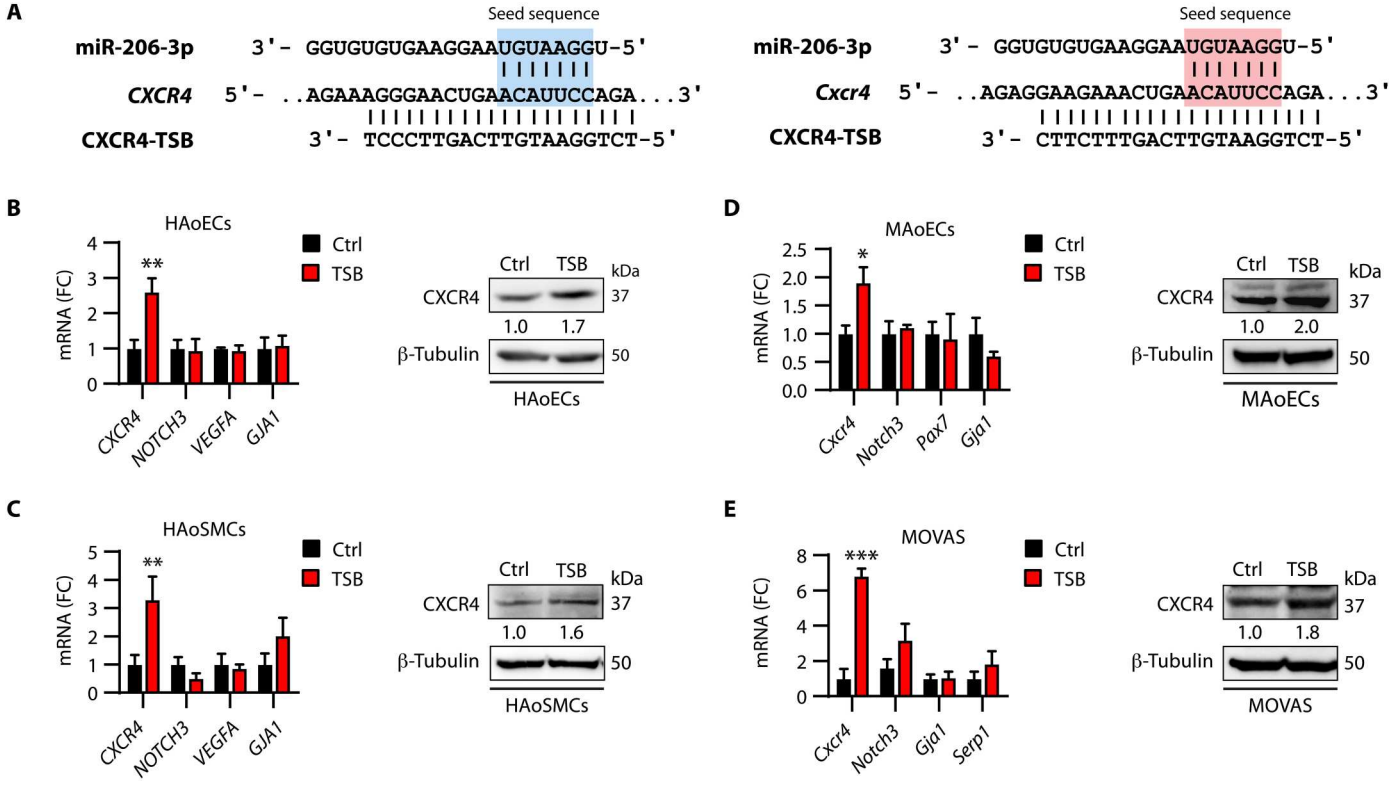

Fig. 2. Design and validation of selective CXCR4 target site blockers (TSB). (**A**) Sequences of miR-206-3p and the binding sites of its seed sequence in the 3′UTR of human (left) and murine (right) *CXCR4* transcripts. The sequence of the TSB and the Watson-Crick pairing with the *CXCR4* transcript is reported below. (**B** to **E**) Functional validation of transfection of CXCR4-TSB (TSB) in HAoECs (B) and HAoSMCs (C) as well as in MAoECs (D) and MOVAS (E). Immunoblotting representative of three independent experiments and quantification of CXCR4 at the mRNA level by qPCR are shown. Additional miR-206-3p targets were assessed by qPCR as negative controls for CXCR4-TSB specificity (n = 4 to 8). Data are presented as means and SEM and were analyzed by factorial ANOVA with Bonferroni post hoc test. *P < 0.05; **P < 0.01; ***P < 0.001.

higher CXCR4 signals in von Willebrand factor $(vWF)^+$ ECs and α-smooth muscle actin $(SMA)^+$ VSMCs but not in $Mac2^+$ macrophages (Fig. 5B). These results show that CXCR4-TSB can enhance arterial CXCR4 expression under atherogenic conditions.

Having verified the feasibility of a CXCR4-TSB treatment in vivo, we studied its relevance to vessel integrity. Consistent with higher proliferative rates, immunofluorescence staining revealed that the proportion of vWF^+ ECs displaying a nuclear Ki67 staining was increased in mice treated with CXCR4-TSB (Fig. 5C). No discernable staining for Ki67 was observed in the subintimal space, in line with the EC-specific effect on proliferation observed in vitro. Next, we evaluated changes in vascular permeability and found that mice treated with CXCR4-TSB for 4 weeks displayed lower Evans blue extravasation in the aorta, particularly in the athero-susceptible aortic arch (Fig. 5, D and E), as well as in the kidneys and spleen (fig. S5A). This result suggests a benefit of disrupting the miR-206-3p–*CXCR4* interaction for both the macro- and microvasculature. We further studied possible effects on LDL retention and subintimal extravasation as crucial events in early atherogenesis. To this end, we analyzed Dil-labeled LDL (Dil-LDL) retention ex vivo in viable carotid arteries isolated from $Apoe^{-/-}$ mice undergoing a 6-week WD and weekly administration of CXCR4-TSB or control LNA oligonucleotides during the final 4 weeks. As visualized by two-photon laser scanning microscopy (TPLSM), the retention of Dil-LDL was decreased in CXCR4-TSB–treated mice as compared with controls (Fig. 5F). As revealed by four-dimensional confocal microscopy, the subintimal Dil-LDL extravasation was delayed in en face prepared aortas of mice treated with CXCR4-TSB as compared with controls (movies S1 and S2), thus extending the findings to another vascular district. Collectively, these results establish the ability of CXCR4-TSB to preserve vascular integrity and reduce permeability to atherogenic lipoproteins.

Furthermore, we analyzed the effect of CXCR4-TSB on leukocyte adhesion to the endothelium as a surrogate of inflammatory activation and dysfunction. After 2 weeks of WD feeding to promote endothelial activation, $Apoe^{-/-}$ mice were treated with CXCR4-TSB or control scrambled LNA oligonucleotides before isolating carotids for ex vivo arterial perfusion assay (Fig. 6A). As visualized by TPLSM, the adhesion of leukocytes on the endothelium of mounted carotid arteries from mice treated with the CXCR4-TSB was reduced when compared with controls (Fig. 6B). We did not observe any difference when leukocytes isolated from mice treated with CXCR4-TSB were perfused in carotid arteries of mice injected with a control LNA oligonucleotide (Fig. 6B), establishing that changes in adhesion were dependent on effects on the arterial wall rather than leukocytes. Consistent with lower inflammatory activation of ECs, the proportion of intercellular adhesion molecule–1 $(ICAM\text{-}1)^+$ ECs in carotid arteries mounted in an ex vivo perfusion

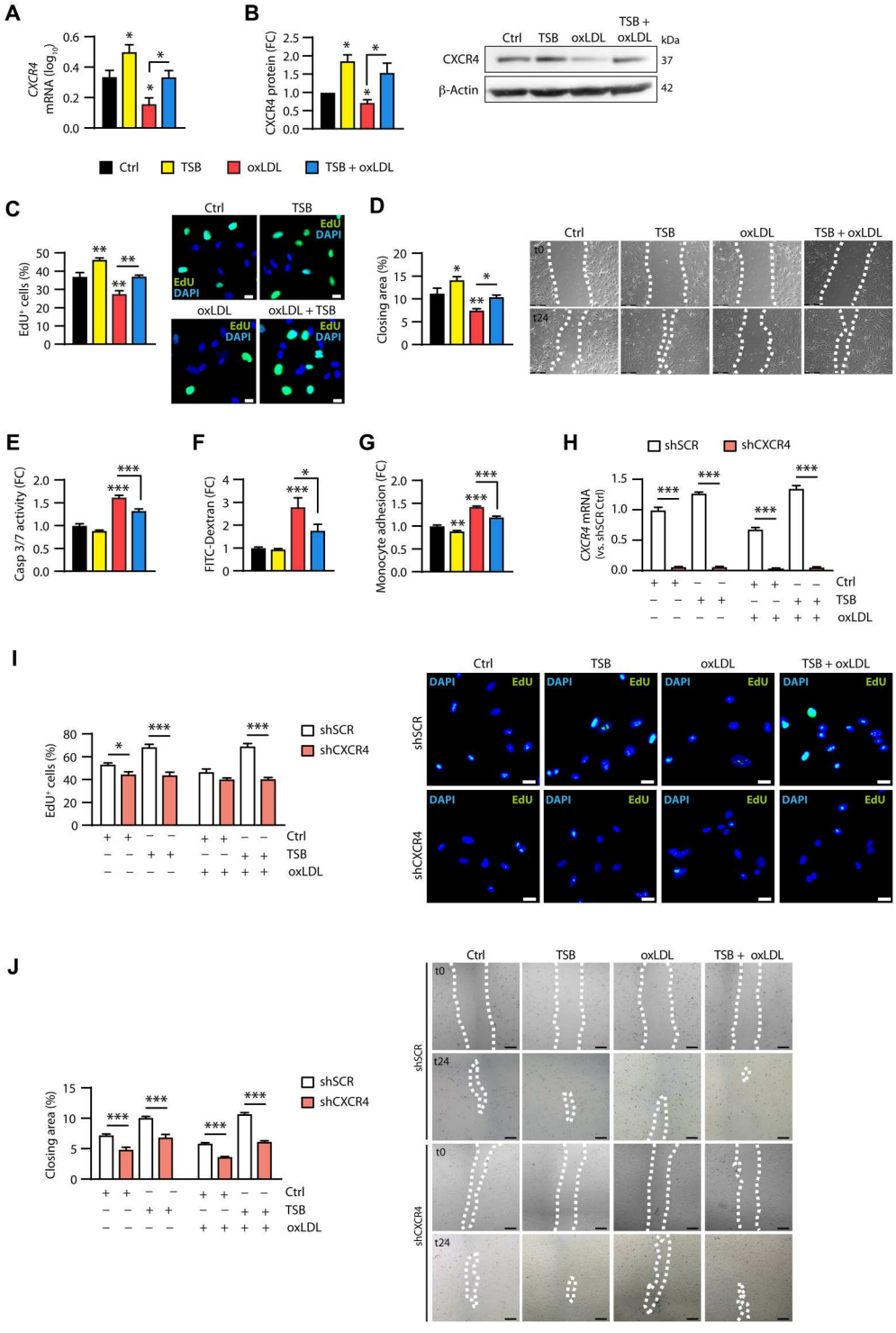

Fig. 3. Functional relevance of disrupting the miR-206-3p–CXCR4 interaction in ECs. (**A** to **G**) HAoECs were transfected with CXCR4-TSB (TSB, 50 nM) or scrambled oligonucleotides (Ctrl) for 48 hours before being treated with or without oxLDL (100 μg/ml) for 24 hours. CXCR4 expression was evaluated at the mRNA (qPCR, A) and protein (Western blot, B) levels ($n = 4$ to 7). Quantification of (C) 5-ethynyl-2′-deoxyuridine (EdU) incorporation to assess proliferation ($n = 4$), (D) wound healing assays to evaluate migration ($n = 7$), (E) caspase-3/7 cleavage assays for apoptosis activation ($n = 5$ or 6), (F) permeability for fluorescein isothiocyanate (FITC)–conjugated dextran ($n = 5$ to 10), and (G) adhesion of calcein-labeled monocytes to the endothelial monolayer normalized to control ($n = 4$). Representative images are provided for (B) to (D). (**H** to **J**) HAoECs were transduced with lentiviral particles expressing shRNAs targeting CXCR4 (shCXCR4) or scrambled controls (shSCR) and transfected with CXCR4-TSB (TSB, 50 nM) or scrambled oligonucleotides (Ctrl) for 48 hours before treatment with or without oxLDL (100 μg/ml) for 24 hours. *CXCR4* expression was evaluated at the mRNA level by qPCR ($n = 5$) (H). Representative images and quantification of wound healing (I) and EdU incorporation (J) assays ($n = 3$ or 4). Scale bars, 10 μm. Data are presented as means and SEM and analyzed by factorial ANOVA with the Bonferroni post hoc test. *$P < 0.05$; **$P < 0.01$; ***$P < 0.001$. DAPI, 4′,6-diamidino-2-phenylindole.

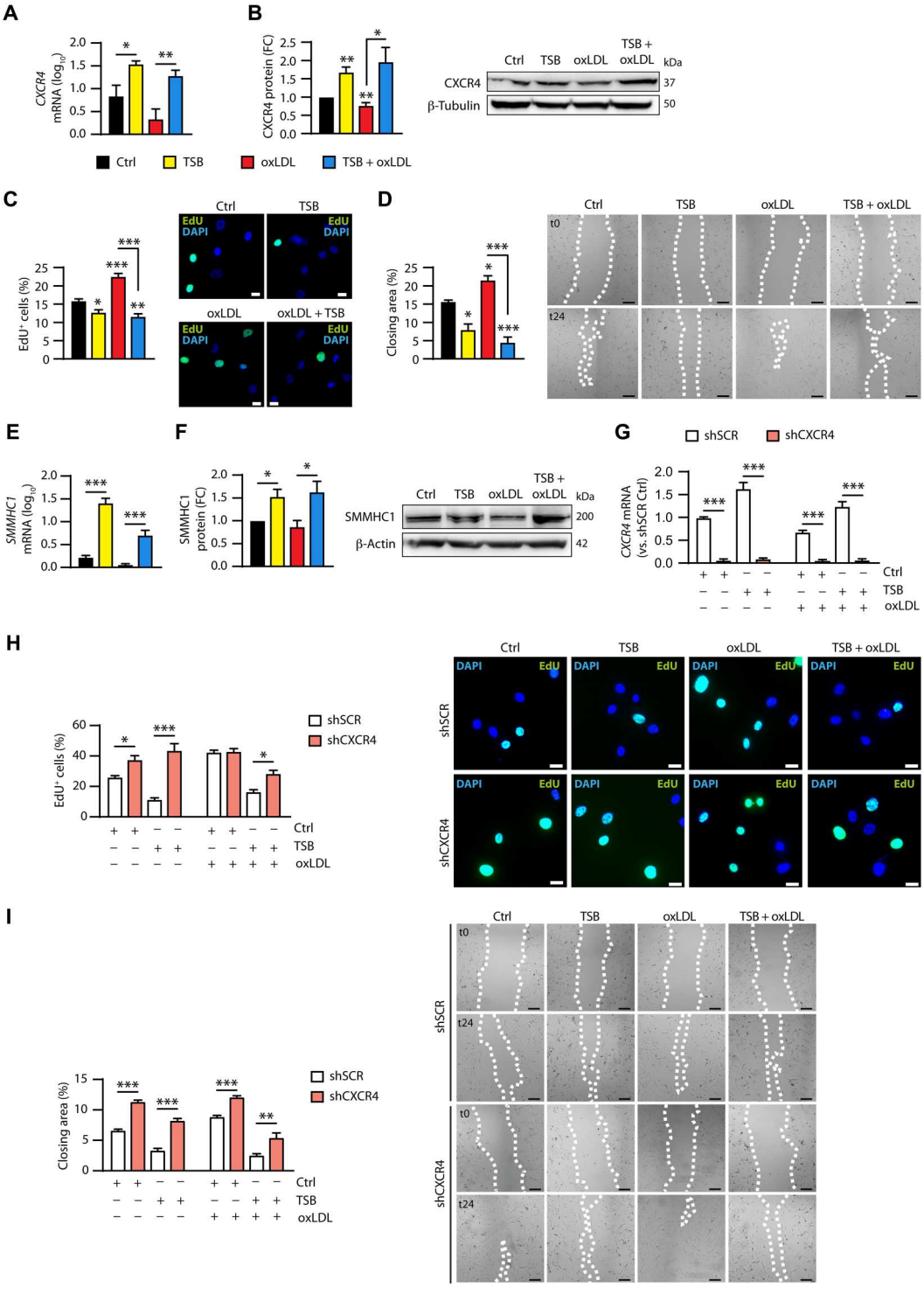

Fig. 4. Functional relevance of disrupting the miR-206-3p–CXCR4 interaction in VSMCs. (**A** to **F**) HAoSMCs were transfected with CXCR4-TSB (TSB, 50 nM) or scrambled oligonucleotides (Ctrl) for 48 hours before being treated with or without oxLDL (100 μg/ml) for 24 hours. CXCR4 expression was measured at the mRNA (qPCR, A) and protein (Western blot, B) levels ($n = 5$ to 8). Quantification and representative images of EdU incorporation assays for proliferation (C) ($n = 5$) and wound healing assays for migration (D) ($n = 3$). SMMHC1 expression was measured at the mRNA (qPCR, E) ($n = 4$) and protein (Western blot, F) levels ($n = 8$), and a representative immunoblotting is provided. (**G** to **I**) HAoSMCs were transduced with lentiviral particles expressing shRNAs targeting CXCR4 (shCXCR4) or scrambled controls (shSCR) and transfected with CXCR4-TSB (TSB, 50 nM) or scrambled oligonucleotides (Ctrl) for 48 hours before treatment with or without oxLDL (100 μg/ml) for 24 hours. *CXCR4* expression was evaluated at the mRNA level by qPCR ($n = 6$) (G). Representative images and quantification of wound healing (H) and EdU incorporation (I) assays ($n = 3$ to 6). Scale bars, 10 μm. Data are presented as means and SEM and analyzed by factorial ANOVA with the Bonferroni post hoc test. *$P < 0.05$; **$P < 0.01$; ***$P < 0.001$.

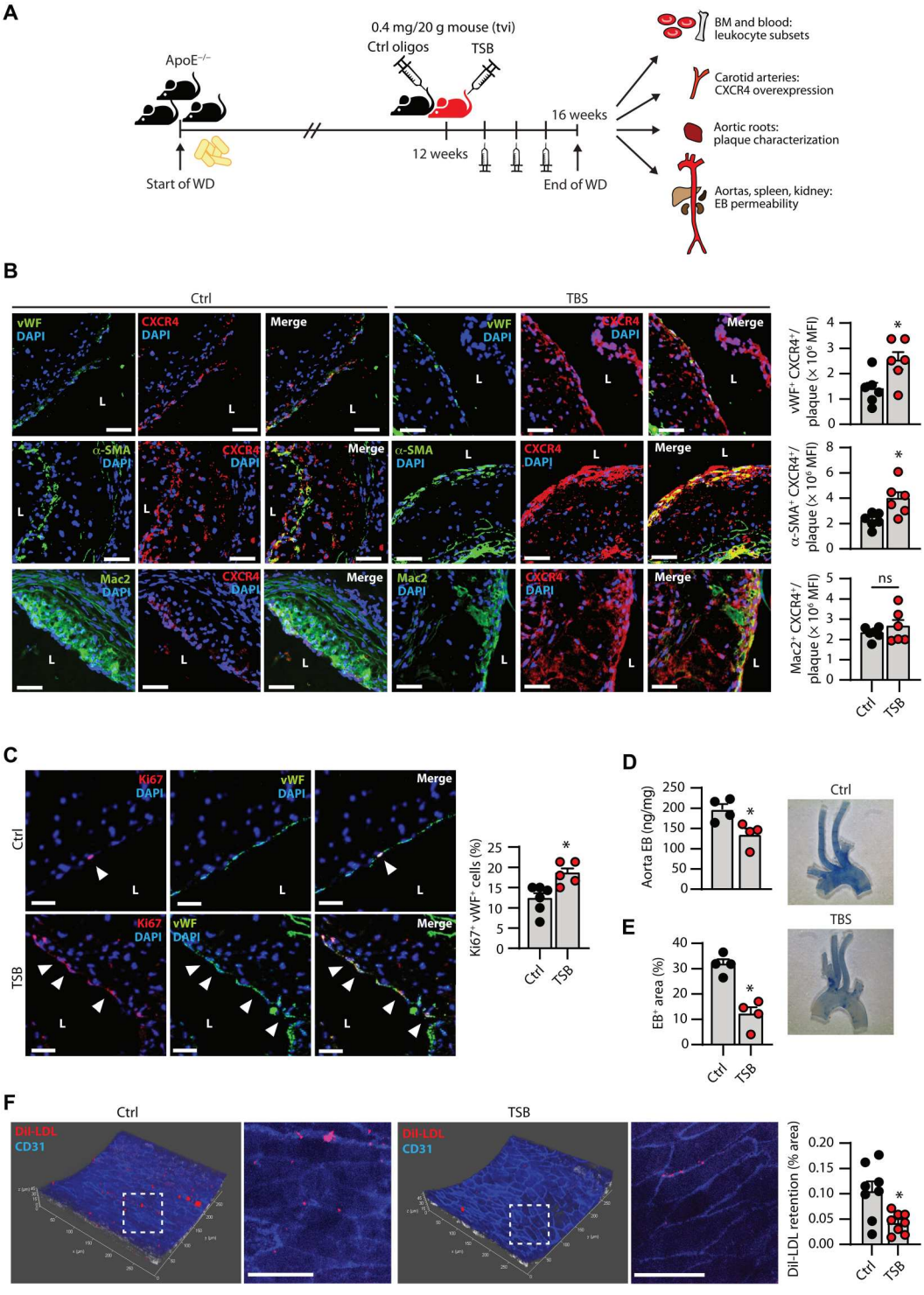

Fig. 5. Assessment of CXCR4-TSB functionality in vivo. (**A**) Experimental layout detailing the treatment plan and tissues collected and analyzed. (**B**) Representative immunofluorescent images and quantification of mean fluorescence intensity (MFI) of CXCR4 signals in aortic roots of *Apoe*$^{-/-}$ mice fed a Western diet (WD) for 16 weeks and treated weekly in the past 4 weeks with CXCR4-TSB (TSB) or scrambled control oligonucleotides (Ctrl). Costaining with vWF, α-SMA, and Mac-2 marks ECs, VSMCs, and macrophages, respectively (n = 6). L, vessel lumen. Scale bars, 50 μm. (**C**) Representative immunofluorescence staining and quantification of the percentage of vWF$^+$ ECs with nuclear staining for the proliferation marker Ki67 in aortic roots of *Apoe*$^{-/-}$ mice treated with CXCR4-TSB (TSB) or scrambled control oligonucleotides (Ctrl) (n = 6). L, vessel lumen. Scale bars, 50 μm. (**D**) Evans blue (EB) extravasation from whole aortas of *Apoe*$^{-/-}$ mice treated with CXCR4-TSB (TSB) or scrambled control oligonucleotides (Ctrl) (n = 4). (**E**) Representative images and quantification of Evans blue extravasation in aortic arches of *Apoe*$^{-/-}$ mice treated with CXCR4-TSB (TSB) or scrambled control oligonucleotides (n = 4). (**F**) Representative images and quantification of the LDL retention assay of DiI-LDL in ex vivo mounted carotid arteries of *Apoe*$^{-/-}$ mice treated with CXCR4-TSB (TSB) or scrambled control oligonucleotides (Ctrl) (n = 8). Scale bars, 50 μm. Data are presented as means and SEM and were analyzed by Student's t test. *P < 0.05; ns, not significant.

chamber as in the leukocyte adhesion assay was strongly reduced in mice treated with CXCR4-TSB (Fig. 6C). Likewise, immunofluorescence staining of atherosclerotic lesions in the aortic root after 16 weeks of WD revealed a lower expression of the adhesion molecule ICAM-1 in mice treated with CXCR4-TSB compared with controls (Fig. 6D). Last, leukocyte recruitment in vivo was assessed by bromodeoxyuridine (BrdU) pulse labeling and short-term intravenous CD45 staining of circulating leukocytes (*40*–*42*). We found that BrdU$^+$CD45$^+$ cells tended to be less abundant in the aortic roots of mice treated with CXCR4-TSB compared with controls (Fig. 6E), in line with the notion that CXCR4 reduces leukocyte trafficking in early atherogenesis by preserving endothelial integrity. This was further corroborated by the ability of CXCR4-TSB to attenuate *Icam1* expression in the presence of oxLDL in MAoECs in

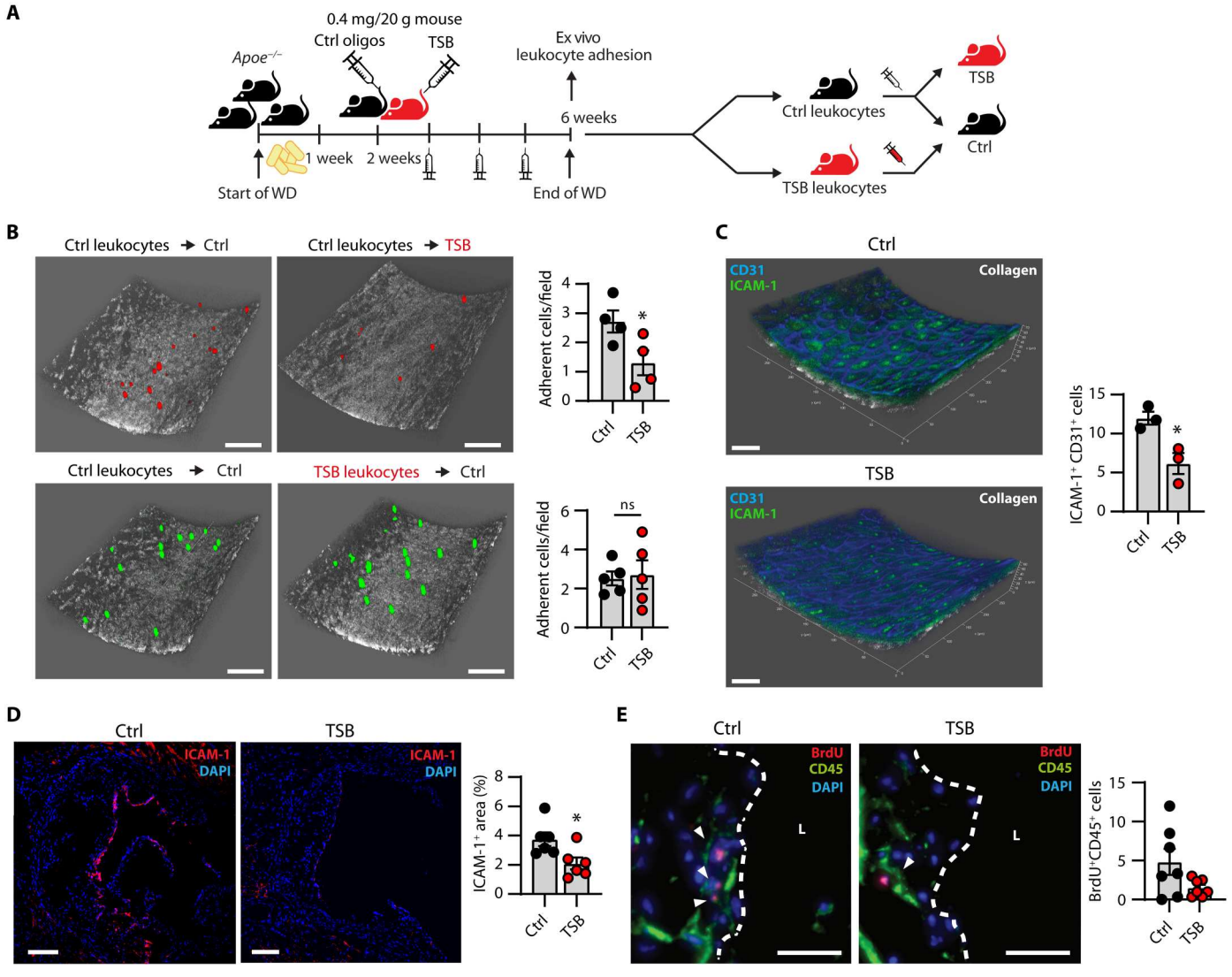

Fig. 6. Assessment of CXCR4-TSB on leukocyte adhesion and recruitment. (**A** to **C**) Experimental layout (A), representative images, and quantification (B) of monocyte adhesion assays performed by perfusion of fluorescently labeled monocytes in ex vivo ($n = 4$ or 5) and (C) percentage of ICAM-1–positive ECs in mounted carotid arteries of *Apoe*$^{-/-}$ mice treated with CXCR4-TSB (TSB) or scrambled control oligonucleotides (Ctrl) ($n = 3$). Scale bars, 50 μm. (**D**) Representative immunostaining and quantification of ICAM-1 protein expression in aortic roots of *Apoe*$^{-/-}$ mice treated with CXCR4-TSB (TSB) or scrambled control oligonucleotides (Ctrl) ($n = 6$). Scale bars, 50 μm. (**E**) Representative images and quantification of leukocyte recruitment in the aortic root in vivo upon BrdU pulse labeling and short-term intravenous CD45 staining of *Apoe*$^{-/-}$ mice treated with CXCR4-TSB (TSB) or scrambled control oligonucleotides (Ctrl) ($n = 7$). Scale bars, 50 μm. Data are presented as means and SEM and were analyzed by Student's *t* test. *$P < 0.05$.

vitro while increasing VE-cadherin expression (fig. S5B), a major determinant of endothelial integrity affected by *Cxcr4* deletion in ECs (*8*). Collectively, these results establish the potential of CXCR4-TSB to reduce endothelial inflammatory activation as well as leukocyte adhesion and their recruitment to atherosclerotic lesions, likely reflecting preserved EC integrity.

CXCR4-TSB enhances CXCR4 expression in B cells but not in other leukocytes

The expression of CXCR4 is ubiquitous, and the CXCR4-CXCL12 axis is instrumental for hematopoietic cell mobilization and homeostasis in the bone marrow. Although we designed CXCR4-TSB to enhance CXCR4 expression in vascular cells but not in monocytes/macrophages, we investigated whether miR-206-3p can also affect CXCR4 expression in other circulating cells. We assessed the surface expression of CXCR4 of the major leukocyte subsets in peripheral blood and bone marrow by flow cytometry and found that treatment of mice with CXCR4-TSB did not affect CXCR4 expression in classical and nonclassical monocytes, T cells, or neutrophils but increased CXCR4 expression in B cells (fig. S6A, B). Similarly, we found that treatment with CXCR4-TSB increased *CXCR4* expression in primary human B cells (fig. S6C), validating the data obtained in mice. Hence, we investigated the effects of CXCR4-TSB on the homeostasis of this cell population. By flow cytometry, we measured higher counts for B cells in peripheral blood and bone marrow of mice treated with CXCR4-TSB compared with

controls (fig. S6, D and E), whereas no differences were found for the other main leukocytes (fig. S6, F and G). We next explored the B cell content in the spleen and found that, whereas the overall number of B cells was unaltered, the counts of marginal B cells were markedly reduced (fig. S6H), possibly suggesting their release into the circulation. CXCR4 in B cells is antiatherogenic and enhances the release of immunoglobulin M (IgM) preventing oxLDL uptake in macrophages (*43*). Consistent with the functional role of CXCR4-TSB, we detected a higher proportion of circulating B1a (but not B1b) cells (fig. S6I), the major source of atheroprotective IgM, and a higher concentration of plasma IgM by enzyme-linked immunoassay (fig. S6J). Last, analysis of plasma concentration of a set of inflammatory cytokines and chemokines in *Apoe*$^{-/-}$ mice treated with CXCR4-TSB did not reveal substantial differences as compared to controls (fig. S6K), ruling out an influence on systemic inflammation and further supporting the specific functional role in the arterial wall. Together, these results confirm that CXCR4-TSB does not affect CXCR4 expression in most leukocyte populations but promotes the increase of CXCR4 expression in B cells, favoring the release of atheroprotective IgM.

CXCR4-TSB reduces diet-induced atherosclerosis in vivo

Our results indicated the feasibility of targeting the miR-206-3p–*Cxcr4* interaction for therapeutic purposes against atherosclerosis. Hence, we used a model of diet-induced atherosclerosis by feeding *Apoe*$^{-/-}$ mice a WD for 6, 12, and 16 weeks. During the last 4 weeks before tissue harvesting, we injected CXCR4-TSB or control scrambled LNA oligonucleotides (0.4 mg/20 g mouse) weekly (Fig. 7A). At every time point, a lower burden of atherosclerosis was detected in the aortic roots of mice treated with CXCR4-TSB as compared with controls (Fig. 7B), yet the temporal trend revealed a slower progression rather than disease regression. At the most advanced time point (16 weeks), CXCR4-TSB effectively increased the expression of *Cxcr4* in the arterial wall, as assessed by qPCR on RNA isolated from carotid arteries (fig. S7A). Although CXCR4-TSB treatment did not alter body weight (fig. S7B), plasma triglyceride, and cholesterol concentrations (fig. S7, C and D), a lower plaque area was detected in en face prepared aortas stained with Sudan IV (Fig. 7B) compared with controls. These results establish the efficacy of CXCR4-TSB in reducing the progression of atherosclerosis without affecting metabolic and lipid profiles.

Next, we analyzed the composition of atherosclerotic plaques upon treatment with CXCR4-TSB. When compared with controls, mice treated with CXCR4-TSB displayed a lower extent of Oil Red O staining (Fig. 7C), indicative of reduced lipid accumulation in lesional foam cells, and smaller necrotic cores (Fig. 7F). In line with improved vascular integrity driven by CXCR4 (*8*), the number of Mac2^{+} macrophages was lower in mice treated with CXCR4-TSB than in controls (Fig. 7E), likely reflecting attenuated leukocyte recruitment. Conversely, no differences were observed in the collagen area assessed by Masson's trichrome staining (Fig. 7F) or in the number of αSMA^{+} VSMCs (Fig. 7G), consistent with the maintenance of a quiescent VSMC phenotype. Together, our results illustrate the therapeutic potential of CXCR4-TSB in limiting the progression of atherosclerosis and the inflammatory burden in the lesions.

The miR-206-3p–CXCR4 interaction occurs in human atherosclerosis

To gain insights into the involvement of miR-206-3p and CXCR4 in human vascular disease, we performed fluorescence in situ hybridization (FISH) to analyze miR-206-3p expression and coimmunostaining for CXCR4 and the EC marker CD31 in human atherosclerotic lesions obtained by thrombendarteriectomy for high-grade stenosis of internal carotid arteries. To infer a possible contribution to atheroprogression, we measured the expression of CXCR4 and miR-206-3p in slices with limited pathological evidence of disease [early lesion area (ELA)] and compared them with areas with the highest atherosclerotic burden [advanced lesion area (ALA)]. We found that advanced plaque areas showed higher miR-206-3p expression, with signals mainly located in the endothelial layer and the subintimal space, whereas the expression of CXCR4 was reduced and limited to a few ECs (Fig. 8). In contrast, early plaque areas displayed stronger signals for CXCR4, mainly localizing to the endothelium, whereas miR-206-3p was hardly detectable (Fig. 8). An inverse bivariate correlation between the expression of miR-206-3p and that of CXCR4 was computed (Spearman's rho −0.62, $P = 0.048$), supporting a repressive function of miR-206-3p on CXCR4 in human atherosclerotic plaques. Together, our results provide evidence for the notion that the miR-206-3p–CXCR4 interaction is operative in mouse and human atherosclerosis and that this pathway may be targeted with a CXCR4-TSB for therapeutic purposes.

DISCUSSION

We demonstrate the beneficial effects of enhancing the expression of CXCR4 in vascular cells as a suitable therapeutic approach for atherosclerosis and potentially other vascular diseases. The role of CXCR4 (and its native ligand CXCL12) in cardiovascular disease and atherosclerosis in humans is strongly supported by genetic association studies (*8*, *9*, *44*, *45*), suggesting exploitation for therapeutic purposes. Yet the intricate network of contrasting functions of the CXCR4-CXCL12 axis in different cell types (*8*, *10*–*13*) and its involvement in bone marrow homeostasis and stem cell mobilization (*46*, *47*) require strategies for tailored expression of *CXCR4* exclusively in vascular cells. Therapeutic gene delivery can be achieved with viral vectors [for instance, with adeno-associated viruses (AAVs)], which received approval for the treatment of rare genetic diseases (*48*, *49*). However, directing the transgene expression toward specific cell types remains a major technical challenge, and transduction of the arterial vessel wall is affected by low-efficiency rates (*49*–*51*). In our study, we proposed and validated an alternative approach based on RNA therapeutics. To address the challenge of cell-specifically enhancing gene expression upon systemic administration, we aimed to disrupt the interaction between *CXCR4* mRNA and miRNAs preferentially expressed in the cells to be targeted, in our case miR-206-3p. miRNA expression is highly cell specific, and studies of human cell lines found that 29% of the miRNAs are unique to a single class of cells (*52*, *53*). This specificity is conferred by the location of *MIRNA* genes in proximity to active cell-specific superenhancers, genomic regions strongly enriched with binding sites for transcription factors with multiplicative effects on the transcription of adjacent genes (*18*, *53*). Although atherogenic stimuli affect the expression of mature miRNAs, they do not influence the use of transcription start sites (TSSs) and

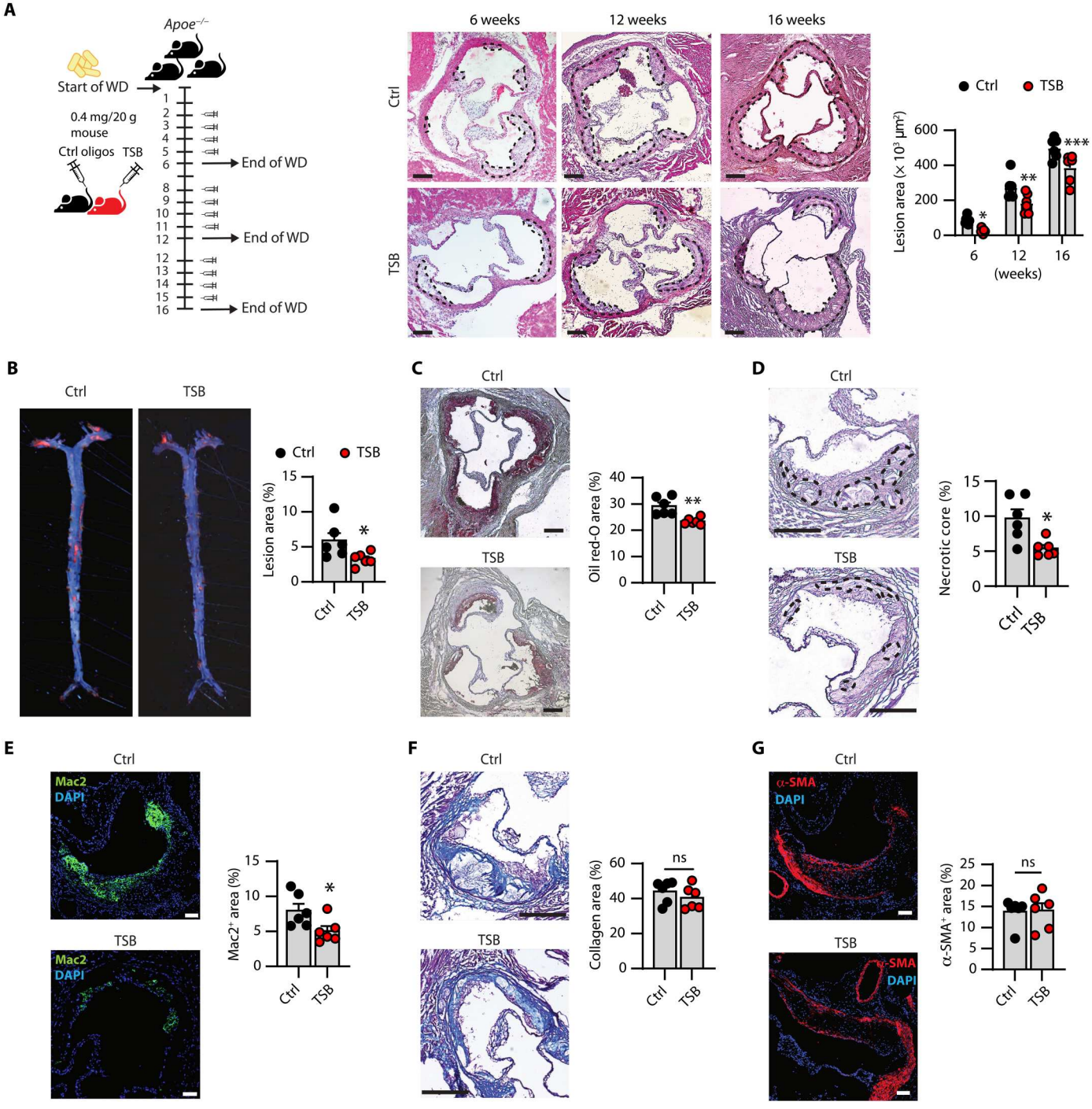

Fig. 7. CXCR4-TSB reduces diet-induced atherosclerosis. (**A**) Experimental layout detailing the diet and treatment plan, with representative hematoxylin and eosin staining of aortic roots and quantification of the atherosclerotic lesion area of *Apoe*$^{-/-}$ mice fed a WD for 6, 12, and 16 weeks and treated with CXCR4-TSB (TSB) or scrambled oligonucleotides (Ctrl) during the last 4 weeks (n = 6 to 8). Scale bars, 100 µm. (**B**) Representative images and quantification of Sudan IV staining on en face aortas of *Apoe*$^{-/-}$ mice fed a WD for 16 weeks and treated with CXCR4-TSB (TSB) or scrambled oligonucleotides (Ctrl) during the past 4 weeks (n = 6). Scale bars, 300 µm. (**C**) Oil Red O staining of aortic roots and quantification of lipid deposition (n = 6). Scale bars, 100 µm. (**D**) Representative hematoxylin and eosin staining of aortic roots and quantification of the necrotic core (n = 6). Scale bars, 50 µm. (**E**) Immunofluorescence staining of the macrophage marker Mac2 in aortic root plaques and quantification of the Mac2^{+} area (n = 6). Scale bars, 100 µm. (**F**) Masson's trichrome staining of aortic roots and quantification of the collagen area in atherosclerotic lesions (n = 6). Scale bars, 50 µm. (**G**) Immunofluorescence staining for the VSMC marker αSMA of atherosclerotic plaques in aortic roots and quantification (n = 6). Data are presented as means and SEM and were analyzed by factorial ANOVA with the Bonferroni post hoc test (A) or by Student's t test (B to G). *P < 0.05; **P < 0.01; ***P < 0.001. ns, not significant.

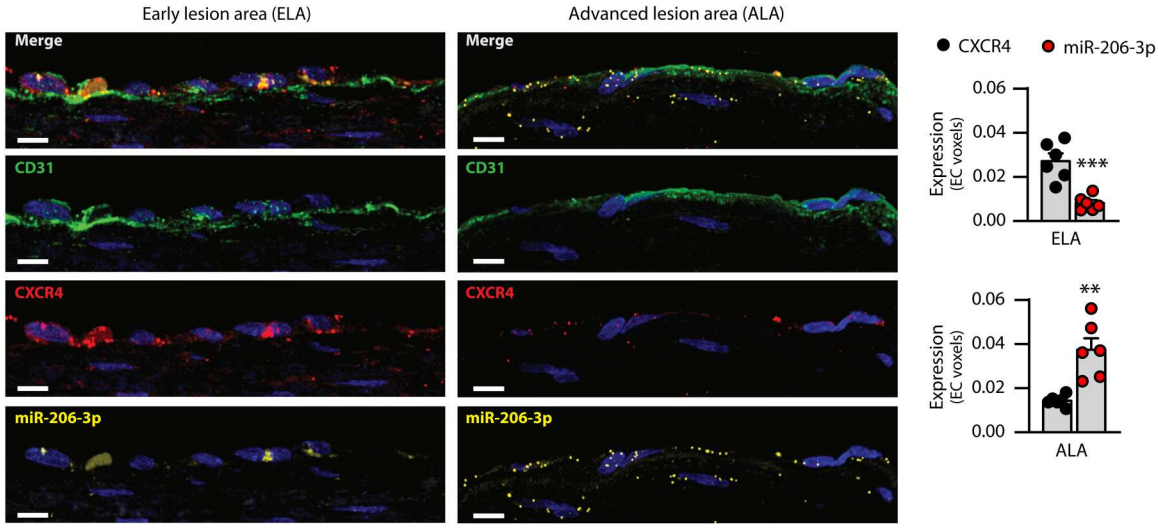

Fig. 8. The miR-206-3p–CXCR4 regulatory interaction is conserved in human atherosclerosis. Representative fluorescent in situ hybridization (FISH) on human carotid atherosclerotic plaques with coimmunostaining for CXCR4 and the EC marker CD31. Quantification of fluorescent signals for CXCR4 and miR-206-3p is reported for early (ELA) and advanced lesion areas (ALA) ($n = 6$). Scale bars, 10 μm. Data are presented as means and SEM and analyzed by Student's t test. $^{**}P < 0.01$; $^{***}P < 0.001$.

pri-miRNA transcription (*18*). Thus, cell-specific miRNAs are unlikely to undergo major transcriptional changes under atherogenic conditions, but differences in miRNA expression are rather determined at the posttranscriptional level (*18*, *20*). For this reason, our workflow for identifying the best candidate was based on the CAGE-seq data from the FANTOM5 consortium (*31*), which provides effective genome-wide transcriptional profiling and quantifies the TSS (*31*, *32*). RNA therapeutics are rapidly and cost-effectively produced and emerged as powerful treatment strategies with a rapid transition toward clinical applications, as shown by the mRNA vaccines against severe acute respiratory syndrome coronavirus 2 (*54*, *55*) or the small interfering RNA targeting PCSK9 (inclisiran) (*56*). For CXCR4-TSB, we used LNA-modified oligonucleotides, which are naturally taken up by cells, with a fully phosphorothioate-modified backbone that makes them resistant to ribonuclease-mediated degradation (*26*, *57*). Our study supports this approach as an alternative to viral vectors, and we achieved the unmet therapeutic feature of boosting the expression of CXCR4 in ECs, VSMCs, and B cells (expressing miR-206-3p) while leaving myeloid cells unaffected.

In addition to providing a promising therapeutic tool, the administration of CXCR4-TSB in vivo corroborated the cell-specific mechanistic relevance of CXCR4 in the processes of atherosclerosis. Whereas genetic deletion of *Cxcr4* in ECs markedly increased atherogenesis by disrupting endothelial integrity and promoting leukocyte recruitment (*8*), we found that CXCR4-TSB can enhance CXCR4 expression in ECs to reduce arterial leakage, cholesterol retention, monocyte adhesion and recruitment in the vessel wall, and ultimately atherogenesis.

An unexpected yet intriguing finding was the existence of a miR-206-3p–*CXCR4* interaction in B cells. The contribution of CXCR4 in this cell type and its relevance in atherogenesis have emerged in recent years (*11*, *12*). CXCR4 has been implicated in bone marrow retention of B1a cells to promote an adequate secretion of atheroprotective IgM (*11*), whereas conditional deletion of *Cxcr4* in B cells (in $Apoe^{-/-}Cd19^{CreERT}Cxcr4^{fl/fl}$) strongly reduced bone marrow content of B1a cells, plasma IgM concentration, and aggravated the development of atherosclerosis (*12*). In line with these findings, CXCR4-TSB was able to increase the retention of B cells in the bone marrow and increase IgM production. Solid evidence supports an atheroprotective role of IgM by showing its ability to target oxidation-specific epitopes on LDLs as well as an inverse association between plasma concentrations of such IgM and cardiovascular disease in humans (*11*, *58*–*61*). Therefore, the effects on B cells are likely to contribute to the overall protective properties of CXCR4-TSB against atherogenesis.

Of note, the protective effects were not associated with changes in the plasma lipid profile, supporting the translational perspective of a lipid-independent therapeutic agent operating in synergy with available lipid-lowering strategies to reduce the residual risk for cardiovascular events in patients with atherosclerosis at high cardiovascular risk, such as patients in need of secondary prevention. To this end, additional preclinical studies in large animal models are warranted to validate the present findings and to address the pharmacokinetics of these compounds before entering development of clinical application in humans.

Although we foresee the perspective of using CXCR4-TSB for therapeutic purposes, some aspects require further investigation. Because we focused our analyses on a set of cell types implicated in atherogenesis, we cannot exclude biologically relevant functions of the miR-206-3p–CXCR4 pathway in other cells and tissue not primarily involved in cardiovascular diseases, such as the skeletal muscle. Moreover, the contribution of B cells and IgM to the antiatherosclerotic features of CXCR4-TSB as well as the underlying mechanisms and additional effects on the immunoglobulin repertoire remain to be clarified at this stage. Future studies in transgenic models, such as B cell–deficient $\mu MT^{-/-}$ mice (*62*), will be required to dissect the functional relevance of this cell subset. Last, we show that CXCR4-TSB limited the progression of atherosclerosis but did not result in regression of established disease. Thus, it would be warranted to assess whether higher doses or prolonged treatment may further enhance the therapeutic potential of CXCR4-TSB in a quest

to define the optimal therapeutic window for possible clinical applications.

In conclusion, disengagement of miRNA-mediated gene repression represents an attractive, feasible, and cost-effective strategy to promote and fine-tune gene expression at a cell-specific level. Ultimately, this approach might revolutionize current viral-based gene delivery approaches by providing an RNA-based targeting strategy with implications for the development of therapeutics to treat cardiovascular disease and beyond.

MATERIALS AND METHODS

Study design

The main objective of our study was to identify a miRNA-CXCR4 regulatory axis operating in cells of the arterial wall (ECs and VSMCs) to selectively disrupt it and to specifically boost CXCR4 expression in these cells. Because miRNAs exhibit remarkable cell-specific transcription, we took advantage of available CAGE-seq databases to identify miRNAs, which can regulate CXCR4 and are transcribed in arterial vessels but not in myeloid cells. Experiments in vitro in murine and human ECs, VSMCs, and macrophages involved gain- and loss-of-function approaches and luciferase report assays to validate the effective regulatory activity of the candidate miRNAs. To disrupt the interaction of the strongest candidate (miR-206-3p) with *CXCR4* mRNA, we used a short oligonucleotide and (i) assessed the functional role on proliferation, migration, apoptosis, and inflammatory activation in murine and human cells in vitro; (ii) confirmed the functional relevance and the neutral effect on leukocytes in an atheroprone mouse model in vivo; and (iii) determined the potential of therapeutic use in a mouse model of advanced diet-induced atherosclerosis. Last, we tested the conservation of this pathway in human atherosclerosis by associative analyses between miR-206-3p and CXCR4 in human atherosclerotic lesions with different severity. For animal experiments, mice were randomized to the different experimental groups, and an a priori calculation of power based on previous data in literature and pilot experiments was performed that aimed at 80% statistical power for detecting biological relevant changes (50%) with a two-tailed α value of 0.05. Animals were excluded from analyses only in the presence of severe health issues. For in vitro experiments, sample sizes were selected empirically on the basis of pilot experiments. Quantification of immunostaining was performed in a blinded manner.

In vitro experiments

Experiments were performed on MAoECs (PB-C57-6052, PELO-Biotech), HAoECs (C-12271, PromoCell), MOVAS [CRL-2797, American Type Culture Collection (ATCC)], HAoSMC (C-12533, PromoCell), BMDMs isolated from mice and differentiated with L929 conditioned medium and macrophage colony-stimulating factor, THP-1 (TIB-202, ATCC) differentiated into macrophages by incubation with PMA (Sigma-Aldrich), and primary mouse B cells isolated with a B cell isolation kit (Miltenyi Biotec) from single-cell spleen suspensions. All cell types were grown using cell-specific culture medium (details in Supplementary Materials and Methods) supplemented with 1% penicillin-streptomycin at 37°C in a humidified atmosphere containing 5% CO_2. Cells were transfected with antisense LNA GapmeRs designed against *DICER1*, miRCURY LNA miR-206-3p inhibitors or mimics, CXCR4-TSB, or scrambled oligonucleotides (all 50 nM, Qiagen) using Lipofectamine 2000 (Thermo Fisher Scientific). The sequences of the transfected oligonucleotides are listed in table S2.

RNA was isolated using RNeasy Mini or miRNeasy mini kits (Qiagen). The expression of miRNAs was assessed using the miScript workflow (Qiagen) following the manufacturer's protocol. The expression of mRNA was measured by reverse-transcribing RNA into complementary DNA with a QuantiTect reverse transcription kit (Qiagen) and performing qPCR with the GoTaq qPCR Master Mix (Promega) and custom-designed primers (table S3) on the QuantStudio 6 Pro Real-Time PCR System (Applied Biosystems). Protein extraction was accomplished with a mammalian protein extraction reagent (M-PER) or a radioimmunoprecipitation assay (RIPA) buffer supplemented with protease (cOmplete protease inhibitor cocktail, Roche) and phosphatase inhibitors (PhosSTOP, Roche), and concentration was measured by a detergent compatible (DC) protein assay (Bio-Rad). For immunoblotting, 15 to 30 μg of proteins was resolved in 4 to 12% Bis-Tris NuPage gels and transferred to Immobilon-E polyvinylidene difluoride (PVDF) membranes (Merck). Membranes were incubated with primary antibodies overnight at 4°C, followed by 1-hour incubation with horseradish peroxidase (HRP)–conjugated secondary antibodies before detection using SuperSignal West Pico Chemiluminescent Substrate (Thermo Fisher Scientific). The list of antibodies used in the study is reported in table S4.

Functional assays probed (i) permeability by analyzing the passage of fluorescein isothiocyanate (FITC)–labeled dextran through a monolayer of ECs seeded onto collagen-coated inserts, (ii) wound healing by testing the ability of EC and VSMC monolayers to recover confluency after experimental scratch damage, (iii) apoptosis by measuring caspase-3/7 enzymatic activity with a Caspase-Glo 3/7 assay (Promega), (intravenously) 5-ethynyl-2′-deoxyuridine (EdU) incorporation by treating ECs and VSMCs with EdU for 12 hours followed by immunostaining for EdU (Click-iT EdU imaging kit, Merck Millipore), and (v) adhesion of fluorescently labeled THP-1 cells incubated over a monolayer of ECs measured as fluorescence intensity in a microplate reader (Tecan Infinite 200 PRO) after three washing steps. Detailed experimental protocols are provided in Supplementary Materials and Methods.

Ex vivo arterial perfusion assay

Carotid arteries isolated from *Apoe*$^{-/-}$ mice treated with CXCR4-TSB or scrambled oligonucleotides were mounted in a home-built perfusion chamber and visualized by TPLSM as previously described (*63*). Arteries were pressurized to 80 mmHg, labeled with anti-CD31 antibody to visualize EC junctions, and perfused for 10 min at a flow rate of 0.54 ml/min (mimicking the in vivo arterial flow rate) with fluorescently labeled leukocytes [Cell Tracker Green/5-chloromethylfluorescein diacetate (CMFDA) or Deep Red; Thermo Fisher Scientific]. Counting of adhesive cells was manually performed in real time using XYZ scans. Subsequently, representative three-dimensional image datasets were recorded and processed using the Leica Application Suite for Advanced Fluorescence (LAS AF) software. For the LDL retention assay, Dil-LDL was intraluminally infused in mounted and pressurized carotid arteries and incubated for 90 min. Thereafter, arteries were flushed to remove free Dil-LDL, labeled with anti-CD31 antibody to visualize EC junctions, and visualized by TPLSM.

In vivo experiments

All animal experiments were reviewed and approved by the local authorities (District Government of Upper Bavaria, Germany) following German animal protection laws. Atheroprone 6- to 8-week-old *Apoe*$^{-/-}$ mice (the Jackson Laboratory) were fed a WD (21% crude fat, 0.15% cholesterol, and 19.5% protein) for 6, 12, or 16 weeks and randomized to treatment with CXCR4-TSB or control LNA oligonucleotides (miRCURY LNA TSB for in vivo use, Qiagen) (0.4 mg/20 g, intravenously) during the last 4 weeks. Once euthanized, CXCR4 expression was studied in the arterial wall and in atherosclerotic lesions by immunofluorescence and in leukocytes by flow cytometry. Assessment of atherosclerotic burden and characterization of plaques was performed in en face prepared aortas and aortic roots. Vascular permeability was assessed by Evans blue extravasation. Intraplaque leukocyte recruitment in vivo was assessed upon BrdU pulse labeling and short-term intravenous anti-CD45 staining of circulating leukocytes. A comprehensive and more detailed description of all experimental procedures can be found in the Supplementary Materials.

Statistical analysis

Data were analyzed using Prism 10 (GraphPad Inc.). Descriptive statistics included mean and SEM unless differently indicated. Data distribution and homogeneity of variance were tested by the Shapiro-Wilk and Levene's tests, respectively. Comparisons between two groups were performed by Student's *t* test, with Welch correction as appropriate, or Mann-Whitney *U* test. Univariate or factorial analysis of variance (ANOVA) with the Bonferroni post hoc test was used to assess the significance of comparisons among three or more groups. The statistical tests and the *n* values, referring to biological replicates in at least two independent experiments, are reported in the figure legends. Differences were deemed significant at two-tailed $P < 0.05$.

Supplementary Materials

This PDF file includes:
Materials and Methods
Figs. S1 to S7
Tables S1 to S4
References (*64*–*79*)

Other Supplementary Material for this manuscript includes the following:
Movies S1 and S2
Data file S1
MDAR Reproducibility Checklist

REFERENCES AND NOTES

1. C. Weber, H. Noels, Atherosclerosis: Current pathogenesis and therapeutic options. *Nat. Med.* **17**, 1410–1422 (2011).
2. G. A. Roth, G. A. Mensah, C. O. Johnson, G. Addolorato, E. Ammirati, L. M. Baddour, N. C. Barengo, A. Z. Beaton, E. J. Benjamin, C. P. Benziger, A. Bonny, M. Brauer, M. Brodmann, T. J. Cahill, J. Carapetis, A. L. Catapano, S. S. Chugh, L. T. Cooper, J. Coresh, M. Criqui, N. DeCleene, K. A. Eagle, S. Emmons-Bell, V. L. Feigin, J. Fernandez-Sola, G. Fowkes, E. Gakidou, S. M. Grundy, F. J. He, G. Howard, F. Hu, L. Inker, G. Karthikeyan, N. Kassebaum, W. Koroshetz, C. Lavie, D. Lloyd-Jones, H. S. Lu, A. Mirijello, A. M. Temesgen, A. Mokdad, A. E. Moran, P. Muntner, J. Narula, B. Neal, M. Ntsekhe, G. Moraes de Oliveira, C. Otto, M. Owolabi, M. Pratt, S. Rajagopalan, M. Reitsma, A. L. P. Ribeiro, N. Rigotti, A. Rodgers, C. Sable, S. Shakil, K. Sliwa-Hahnle, B. Stark, J. Sundstrom, P. Timpel, I. M. Tleyjeh, M. Valgimigli, T. Vos, P. K. Whelton, M. Yacoub, L. Zuhlke, C. Murray, V. Fuster; GBD-NHLBI-JACC Global Burden of Cardiovascular Diseases Writing Group, Global burden of cardiovascular diseases and risk factors, 1990–2019: Update from the GBD 2019 study. *J. Am. Coll. Cardiol.* **76**, 2982–3021 (2020).
3. T. Vos, S. S. Lim, C. Abbafati, K. M. Abbas, M. Abbasi, M. Abbasifard, M. Abbasi-Kangevari, H. Abbastabar, F. Abd-Allah, A. Abdelalim, M. Abdollahi, I. Abdollahpour, H. Abolhassani, V. Aboyans, E. M. Abrams, L. G. Abreu, M. R. M. Abrigo, L. J. Abu-Raddad, A. I. Abushouk, A. Acebedo, I. N. Ackerman, M. Adabi, A. A. Adamu, O. M. Adebayo, V. Adekanmbi, J. D. Adelson, O. O. Adetokunboh, D. Adham, M. Afshari, A. Afshin, E. E. Agardh, G. Agarwal, K. M. Agesa, M. Aghaali, S. M. K. Aghamir, A. Agrawal, T. Ahmad, A. Ahmadi, M. Ahmadi, H. Ahmadieh, E. Ahmadpour, T. Y. Akalu, R. O. Akinyemi, T. Akinyemiju, B. Akombi, Z. Al-Aly, K. Alam, N. Alam, S. Alam, T. Alam, T. M. Alanzi, Global burden of 369 diseases and injuries in 204 countries and territories, 1990–2019: A systematic analysis for the Global Burden of Disease Study 2019. *Lancet* **396**, 1204–1222 (2020).
4. E. G. Nabel, E. Braunwald, A tale of coronary artery disease and myocardial infarction. *N. Engl. J. Med.* **366**, 54–63 (2012).
5. E. Lutgens, D. Atzler, Y. Doring, J. Duchene, S. Steffens, C. Weber, Immunotherapy for cardiovascular disease. *Eur. Heart J.* **40**, 3937–3946 (2019).
6. C. Weber, A. J. R. Habenicht, P. von Hundelshausen, Novel mechanisms and therapeutic targets in atherosclerosis: Inflammation and beyond. *Eur. Heart J.* **44**, 2672–2681 (2023).
7. K. Tachibana, S. Hirota, H. Iizasa, H. Yoshida, K. Kawabata, Y. Kataoka, Y. Kitamura, K. Matsushima, N. Yoshida, S. Nishikawa, T. Kishimoto, T. Nagasawa, The chemokine receptor CXCR4 is essential for vascularization of the gastrointestinal tract. *Nature* **393**, 591–594 (1998).
8. Y. Döring, H. Noels, E. P. C. van der Vorst, C. Neideck, V. Egea, M. Drechsler, M. Mandl, L. Pawig, Y. Jansen, K. Schroder, K. Bidzhekov, R. T. A. Megens, W. Theelen, B. M. Klinkhammer, P. Boor, L. Schurgers, R. van Gorp, C. Ries, P. J. H. Kusters, A. van der Wal, T. M. Hackeng, G. Gabel, R. P. Brandes, O. Soehnlein, E. Lutgens, D. Vestweber, D. Teupser, L. M. Holdt, D. J. Rader, D. Saleheen, C. Weber, Vascular CXCR4 limits atherosclerosis by maintaining arterial integrity: Evidence from mouse and human studies. *Circulation* **136**, 388–403 (2017).
9. K. G. Aragam, T. Jiang, A. Goel, S. Kanoni, B. N. Wolford, D. S. Atri, E. M. Weeks, M. Wang, G. Hindy, W. Zhou, C. Grace, C. Roselli, N. A. Marston, F. K. Kamanu, I. Surakka, L. M. Venegas, P. Sherliker, S. Koyama, K. Ishigaki, B. O. Asvold, M. R. Brown, B. Brumpton, P. S. de Vries, O. Giannakopoulou, P. Giardoglou, D. F. Gudbjartsson, U. Guldener, S. M. I. Haider, A. Helgadottir, M. Ibrahim, A. Kastrati, T. Kessler, T. Kyriakou, T. Konopka, L. Li, L. Ma, T. Meitinger, S. Mucha, M. Munz, F. Murgia, J. B. Nielsen, M. M. Nothen, S. Pang, T. Reinberger, G. Schnitzler, D. Smedley, G. Thorleifsson, M. von Scheidt, J. C. Ulirsch, J. Biobank, C. V. D. Epic, D. O. Arnar, N. P. Burtt, M. C. Costanzo, J. Flannick, K. Ito, D. K. Jang, Y. Kamatani, A. V. Khera, I. Komuro, I. J. Kullo, L. A. Lotta, C. P. Nelson, R. Roberts, G. Thorgeirsson, U. Thorsteinsdottir, T. R. Webb, A. Baras, J. L. M. Bjorkegren, E. Boerwinkle, G. Dedoussis, H. Holm, K. Hveem, O. Melander, A. C. Morrison, M. Orho-Melander, L. S. Rallidis, A. Ruusalepp, M. S. Sabatine, K. Stefansson, P. Zalloua, P. T. Ellinor, M. Farrall, J. Danesh, C. T. Ruff, H. K. Finucane, J. C. Hopewell, R. Clarke, R. M. Gupta, J. Erdmann, N. J. Samani, H. Schunkert, H. Watkins, C. J. Willer, P. Deloukas, S. Kathiresan, A. S. Butterworth, Discovery and systematic characterization of risk variants and genes for coronary artery disease in over a million participants. *Nat. Genet.* **54**, 1803–1815 (2022).
10. A. Zernecke, I. Bot, Y. Djalali-Talab, E. Shagdarsuren, K. Bidzhekov, S. Meiler, R. Krohn, A. Schober, M. Sperandio, O. Soehnlein, J. Bornemann, F. Tacke, E. A. Biessen, C. Weber, Protective role of CXC receptor 4/CXC ligand 12 unveils the importance of neutrophils in atherosclerosis. *Circ. Res.* **102**, 209–217 (2008).
11. A. Upadhye, P. Srikakulapu, A. Gonen, S. Hendrikx, H. M. Perry, A. Nguyen, C. McSkimming, M. A. Marshall, J. C. Garmey, A. M. Taylor, T. P. Bender, S. Tsimikas, N. E. Holodick, T. L. Rothstein, J. L. Witztum, C. A. McNamara, Diversification and CXCR4-dependent establishment of the bone marrow B-1a cell pool governs atheroprotective IgM production linked to human coronary atherosclerosis. *Circ. Res.* **125**, e55–e70 (2019).
12. Y. Doring, Y. Jansen, I. Cimen, M. Aslani, S. Gencer, L. J. F. Peters, J. Duchene, C. Weber, E. P. C. van der Vorst, B-cell-specific CXCR4 protects against atherosclerosis development and increases plasma IgM levels. *Circ. Res.* **126**, 787–788 (2020).
13. A. Zernecke, A. Schober, I. Bot, P. von Hundelshausen, E. A. Liehn, B. Mopps, M. Mericskay, P. Gierschik, E. A. Biessen, C. Weber, SDF-1α/CXCR4 axis is instrumental in neointimal hyperplasia and recruitment of smooth muscle progenitor cells. *Circ. Res.* **96**, 784–791 (2005).
14. S. Heinz, C. E. Romanoski, C. Benner, C. K. Glass, The selection and function of cell type-specific enhancers. *Nat. Rev. Mol. Cell Biol.* **16**, 144–154 (2015).
15. D. P. Bartel, Metazoan microRNAs. *Cell* **173**, 20–51 (2018).
16. D. Santovito, C. Weber, Non-canonical features of microRNAs: Paradigms emerging from cardiovascular disease. *Nat. Rev. Cardiol.* **19**, 620–638 (2022).
17. L. J. F. Peters, E. A. L. Biessen, M. Hohl, C. Weber, E. P. C. van der Vorst, D. Santovito, Small things matter: Relevance of microRNAs in cardiovascular disease. *Front. Physiol.* **11**, 793 (2020).

18. P. R. Moreau, V. Tomas Bosch, M. Bouvy-Liivrand, K. Ounap, T. Ord, H. H. Pulkkinen, P. Polonen, M. Heinaniemi, S. Yla-Herttuala, J. P. Laakkonen, S. Linna-Kuosmanen, M. U. Kaikkonen, Profiling of primary and mature miRNA expression in atherosclerosis-associated cell types. *Arterioscler. Thromb. Vasc. Biol.* **41**, 2149–2167 (2021).
19. A. Schober, M. Nazari-Jahantigh, Y. Wei, K. Bidzhekov, F. Gremse, J. Grommes, R. T. Megens, K. Heyll, H. Noels, M. Hristov, S. Wang, F. Kiessling, E. N. Olson, C. Weber, MicroRNA-126-5p promotes endothelial proliferation and limits atherosclerosis by suppressing Dlk1. *Nat. Med.* **20**, 368–376 (2014).
20. D. Santovito, V. Egea, K. Bidzhekov, L. Natarelli, A. Mourao, X. Blanchet, K. Wichapong, M. Aslani, C. Brunssen, M. Horckmans, M. Hristov, A. Geerlof, E. Lutgens, M. Daemen, T. Hackeng, C. Ries, T. Chavakis, H. Morawietz, R. Naumann, P. von Hundelshausen, S. Steffens, J. Duchene, R. T. A. Megens, M. Sattler, C. Weber, Noncanonical inhibition of caspase-3 by a nuclear microRNA confers endothelial protection by autophagy in atherosclerosis. *Sci. Transl. Med.* **12**, eaaz2294 (2020).
21. L. Elia, M. Quintavalle, J. Zhang, R. Contu, L. Cossu, M. V. Latronico, K. L. Peterson, C. Indolfi, D. Catalucci, J. Chen, S. A. Courtneidge, G. Condorelli, The knockout of miR-143 and -145 alters smooth muscle cell maintenance and vascular homeostasis in mice: Correlates with human disease. *Cell Death Differ.* **16**, 1590–1598 (2009).
22. K. R. Cordes, N. T. Sheehy, M. P. White, E. C. Berry, S. U. Morton, A. N. Muth, T.-H. Lee, J. M. Miano, K. N. Ivey, D. Srivastava, miR-145 and miR-143 regulate smooth muscle cell fate and plasticity. *Nature* **460**, 705–710 (2009).
23. C. Labbaye, I. Spinello, M. T. Quaranta, E. Pelosi, L. Pasquini, E. Petrucci, M. Biffoni, E. R. Nuzzolo, M. Billi, R. Foa, E. Brunetti, F. Grignani, U. Testa, C. Peschle, A three-step pathway comprising PLZF/miR-146a/CXCR4 controls megakaryopoiesis. *Nat. Cell Biol.* **10**, 788–801 (2008).
24. I. Papangeli, J. Kim, I. Maier, S. Park, A. Lee, Y. Kang, K. Tanaka, O. F. Khan, H. Ju, Y. Kojima, K. Red-Horse, D. G. Anderson, A. F. Siekmann, H. J. Chun, MicroRNA 139-5p coordinates APLNR-CXCR4 crosstalk during vascular maturation. *Nat. Commun.* **7**, 11268 (2016).
25. P. Hartmann, Z. Zhou, L. Natarelli, Y. Wei, M. Nazari-Jahantigh, M. Zhu, J. Grommes, S. Steffens, C. Weber, A. Schober, Endothelial dicer promotes atherosclerosis and vascular inflammation by miRNA-103-mediated suppression of KLF4. *Nat. Commun.* **7**, 10521 (2016).
26. L. Natarelli, C. Geißler, G. Csaba, Y. Wei, M. Zhu, A. di Francesco, P. Hartmann, R. Zimmer, A. Schober, miR-103 promotes endothelial maladaptation by targeting lncWDR59. *Nat. Commun.* **9**, 2645 (2018).
27. Y. Wei, J. Corbalan-Campos, R. Gurung, L. Natarelli, M. Zhu, N. Exner, F. Erhard, F. Greulich, C. Geissler, N. H. Uhlenhaut, R. Zimmer, A. Schober, Dicer in macrophages prevents atherosclerosis by promoting mitochondrial oxidative metabolism. *Circulation* **138**, 2007–2020 (2018).
28. F. Zahedi, M. Nazari-Jahantigh, Z. Zhou, P. Subramanian, Y. Wei, J. Grommes, S. Offermanns, S. Steffens, C. Weber, A. Schober, Dicer generates a regulatory microRNA network in smooth muscle cells that limits neointima formation during vascular repair. *Cell. Mol. Life Sci.* **74**, 359–372 (2017).
29. B. Fromm, T. Billipp, L. E. Peck, M. Johansen, J. E. Tarver, B. L. King, J. M. Newcomb, L. F. Sempere, K. Flatmark, E. Hovig, K. J. Peterson, A uniform system for the annotation of vertebrate microRNA genes and the evolution of the human microRNAome. *Annu. Rev. Genet.* **49**, 213–242 (2015).
30. B. Fromm, D. Domanska, E. Hoye, V. Ovchinnikov, W. Kang, E. Aparicio-Puerta, M. Johansen, K. Flatmark, A. Mathelier, E. Hovig, M. Hackenberg, M. R. Friedlander, K. J. Peterson, MirGeneDB 2.0: The metazoan microRNA complement. *Nucleic Acids Res.* **48**, D132–D141 (2020).
31. D. de Rie, I. Abugessaisa, T. Alam, E. Arner, P. Arner, H. Ashoor, G. Astrom, M. Babina, N. Bertin, A. M. Burroughs, A. J. Carlisle, C. O. Daub, M. Detmar, R. Deviatiiarov, A. Fort, C. Gebhard, D. Goldowitz, S. Guhl, T. J. Ha, J. Harshbarger, A. Hasegawa, K. Hashimoto, M. Herlyn, P. Heutink, K. J. Hitchens, C. C. Hon, E. Huang, Y. Ishizu, C. Kai, T. Kasukawa, P. Klinken, T. Lassmann, C. H. Lecellier, W. Lee, M. Lizio, V. Makeev, A. Mathelier, Y. A. Medvedeva, N. Mejhert, C. J. Mungall, S. Noma, M. Ohshima, M. Okada-Hatakeyama, H. Persson, P. Rizzu, F. Roudnicky, P. Saetrom, H. Sato, J. Severin, J. W. Shin, R. K. Swoboda, H. Tarui, H. Toyoda, K. Vitting-Seerup, L. Winteringham, Y. Yamaguchi, K. Yasuzawa, M. Yoneda, N. Yumoto, S. Zabierowski, P. G. Zhang, C. A. Wells, K. M. Summers, H. Kawaji, A. Sandelin, M. Rehli; FANTOM Consortium, Y. Hayashizaki, P. Carninci, A. R. R. Forrest, M. J. L. de Hoon, An integrated expression atlas of miRNAs and their promoters in human and mouse. *Nat. Biotechnol.* **35**, 872–878 (2017).
32. M. Murata, H. Nishiyori-Sueki, M. Kojima-Ishiyama, P. Carninci, Y. Hayashizaki, M. Itoh, Detecting expressed genes using CAGE. *Methods Mol. Biol.* **1164**, 67–85 (2014).
33. H. Seok, H. Lee, S. Lee, S. H. Ahn, H.-S. Lee, G.-W. D. Kim, J. Peak, J. Park, Y. K. Cho, Y. Jeong, D. Gu, Y. Jeong, S. Eom, E. S. Jang, S. W. Chi, Position-specific oxidation of miR-1 encodes cardiac hypertrophy. *Nature* **584**, 279–285 (2020).
34. L. Elia, R. Contu, M. Quintavalle, F. Varrone, C. Chimenti, M. A. Russo, V. Cimino, L. De Marinis, A. Frustaci, D. Catalucci, G. Condorelli, Reciprocal regulation of microRNA-1 and insulin-like growth factor-1 signal transduction cascade in cardiac and skeletal muscle in physiological and pathological conditions. *Circulation* **120**, 2377–2385 (2009).
35. Y. Zhao, J. F. Ransom, A. Li, V. Vedantham, M. von Drehle, A. N. Muth, T. Tsuchihashi, M. T. McManus, R. J. Schwartz, D. Srivastava, Dysregulation of cardiogenesis, cardiac conduction, and cell cycle in mice lacking miRNA-1-2. *Cell* **129**, 303–317 (2007).
36. A. Bisognin, G. Sales, A. Coppe, S. Bortoluzzi, C. Romualdi, MAGIA2: From miRNA and genes expression data integrative analysis to microRNA–transcription factor mixed regulatory circuits (2012 update). *Nucleic Acids Res.* **40**, W13–W21 (2012).
37. H. Y. Huang, Y. C. Lin, S. Cui, Y. Huang, Y. Tang, J. Xu, J. Bao, Y. Li, J. Wen, H. Zuo, W. Wang, J. Li, J. Ni, Y. Ruan, L. Li, Y. Chen, Y. Xie, Z. Zhu, X. Cai, X. Chen, L. Yao, Y. Chen, Y. Luo, S. LuXu, M. Luo, C. M. Chiu, K. Ma, L. Zhu, G. J. Cheng, C. Bai, Y. C. Chiang, L. Wang, F. Wei, T. Y. Lee, H. D. Huang, miRTarBase update 2022: An informative resource for experimentally validated miRNA-target interactions. *Nucleic Acids Res.* **50**, D222–D230 (2022).
38. A. Janjic, L. E. Wange, J. W. Bagnoli, J. Geuder, P. Nguyen, D. Richter, B. Vieth, B. Vick, I. Jeremias, C. Ziegenhain, I. Hellmann, W. Enard, Prime-seq, efficient and powerful bulk RNA sequencing. *Genome Biol.* **23**, 88 (2022).
39. S. W. Eichhorn, H. Guo, S. E. McGeary, R. A. Rodriguez-Mias, C. Shin, D. Baek, S. H. Hsu, K. Ghoshal, J. Villen, D. P. Bartel, mRNA destabilization is the dominant effect of mammalian microRNAs by the time substantial repression ensues. *Mol. Cell* **56**, 104–115 (2014).
40. C. Winter, C. Silvestre-Roig, A. Ortega-Gomez, P. Lemnitzer, H. Poelman, A. Schumski, J. Winter, M. Drechsler, R. de Jong, R. Immler, M. Sperandio, M. Hristov, T. Zeller, G. A. F. Nicolaes, C. Weber, J. R. Viola, A. Hidalgo, C. Scheiermann, O. Soehnlein, Chronopharmacological targeting of the CCL2-CCR2 axis ameliorates atherosclerosis. *Cell Metab.* **28**, 175–182.e5 (2018).
41. J. Ikeda, C. A. Scipione, S. J. Hyduk, M. G. Althagafi, J. Atif, S. A. Dick, M. Rajora, E. Jang, T. Emoto, J. Murakami, N. Ikeda, H. M. Ibrahim, C. K. Polenz, X. Gao, K. Tai, J. Jongstra-Bilen, R. Nakashima, S. Epelman, C. S. Robbins, G. Zheng, W. L. Lee, S. A. MacParland, M. I. Cybulsky, Radiation impacts early atherosclerosis by suppressing intimal LDL accumulation. *Circ. Res.* **128**, 530–543 (2021).
42. S. N. Zhu, M. Chen, J. Jongstra-Bilen, M. I. Cybulsky, GM-CSF regulates intimal cell proliferation in nascent atherosclerotic lesions. *J. Exp. Med.* **206**, 2141–2149 (2009).
43. P. Srikakulapu, A. Upadhye, F. Drago, H. M. Perry, S. V. Bontha, C. McSkimming, M. A. Marshall, A. M. Taylor, C. A. McNamara, Chemokine receptor-6 promotes B-1 cell trafficking to perivascular adipose tissue, local IgM production and atheroprotection. *Front. Immunol.* **12**, 636013 (2021).
44. Y. Doring, E. P. C. van der Vorst, J. Duchene, Y. Jansen, S. Gencer, K. Bidzhekov, D. Atzler, D. Santovito, D. J. Rader, D. Saleheen, C. Weber, CXCL12 derived from endothelial cells promotes atherosclerosis to drive coronary artery disease. *Circulation* **139**, 1338–1340 (2019).
45. CARDIoGRAMplusC4D Consortium, P. Deloukas, S. Kanoni, C. Willenborg, M. Farrall, T. L. Assimes, J. R. Thompson, E. Ingelsson, D. Saleheen, J. Erdmann, B. A. Goldstein, K. Stirrups, I. R. Konig, J. B. Cazier, A. Johansson, A. S. Hall, J. Y. Lee, C. J. Willer, J. C. Chambers, T. Esko, L. Folkersen, A. Goel, E. Grundberg, A. S. Havulinna, W. K. Ho, J. C. Hopewell, N. Eriksson, M. E. Kleber, K. Kristiansson, P. Lundmark, L. P. Lyytikainen, S. Rafelt, D. Shungin, R. J. Strawbridge, G. Thorleifsson, E. Tikkanen, N. Van Zuydam, B. F. Voight, L. L. Waite, W. Zhang, A. Ziegler, D. Absher, D. Altshuler, A. J. Balmforth, I. Barroso, P. S. Braund, C. Burgdorf, S. Claudi-Boehm, D. Cox, M. Dimitriou, R. Do; DIAGRAM Consortium; CARDIOGENICS Consortium, A. S. Doney, N. El Mokhtari, P. Eriksson, K. Fischer, P. Fontanillas, A. Franco-Cereceda, B. Gigante, L. Groop, S. Gustafsson, J. Hager, G. Hallmans, B. G. Han, S. E. Hunt, H. M. Kang, T. Illig, T. Kessler, J. W. Knowles, G. Kolovou, J. Kuusisto, C. Langenberg, C. Langford, K. Leander, M. L. Lokki, A. Lundmark, M. I. McCarthy, C. Meisinger, O. Melander, E. Mihailov, S. Maouche, A. D. Morris, M. Muller-Nurasyid; MuTHER Consortium, K. Nikus, J. F. Peden, N. W. Rayner, A. Rasheed, S. Rosinger, D. Rubin, M. P. Rumpf, A. Schafer, M. Sivananthan, C. Song, A. F. Stewart, S. T. Tan, G. Thorgeirsson, C. E. van der Schoot, P. J. Wagner; Wellcome Trust Case Control Consortium, G. A. Wells, P. S. Wild, T. P. Yang, P. Amouyel, D. Arveiler, H. Basart, M. Boehnke, E. Boerwinkle, P. Brambilla, F. Cambien, A. L. Cupples, U. de Faire, A. Dehghan, P. Diemert, S. E. Epstein, A. Evans, M. M. Ferrario, J. Ferrieres, D. Gauguier, A. S. Go, A. H. Goodall, V. Gudnason, S. L. Hazen, H. Holm, C. Iribarren, Y. Jang, M. Kahonen, F. Kee, H. S. Kim, N. Klopp, W. Koenig, W. Kratzer, K. Kuulasmaa, M. Laakso, R. Laaksonen, J. Y. Lee, L. Lind, W. H. Ouwehand, S. Parish, J. E. Park, N. L. Pedersen, A. Peters, T. Quertermous, D. J. Rader, V. Salomaa, E. Schadt, S. H. Shah, J. Sinisalo, K. Stark, K. Stefansson, D. A. Tregouet, J. Virtamo, L. Wallentin, N. Wareham, M. E. Zimmermann, M. S. Nieminen, C. Hengstenberg, M. S. Sandhu, T. Pastinen, A. C. Syvanen, G. K. Hovingh, G. Dedoussis, P. W. Franks, T. Lehtimaki, A. Metspalu, P. A. Zalloua, A. Siegbahn, S. Schreiber, S. Ripatti, S. S. Blankenberg, M. Perola, R. Clarke, B. O. Boehm, C. O'Donnell, M. P. Reilly, W. Marz, R. Collins, S. Kathiresan, A. Hamsten, J. S. Kooner, U. Thorsteinsdottir, J. Danesh, C. N. Palmer, R. Roberts, H. Watkins, H. Schunkert, N. J. Samani, Large-scale association analysis identifies new risk loci for coronary artery disease. *Nat. Genet.* **45**, 25–33 (2013).

46. T. Sugiyama, H. Kohara, M. Noda, T. Nagasawa, Maintenance of the hematopoietic stem cell pool by CXCL12-CXCR4 chemokine signaling in bone marrow stromal cell niches. *Immunity* **25**, 977–988 (2006).
47. M. J. Christopher, F. Liu, M. J. Hilton, F. Long, D. C. Link, Suppression of CXCL12 production by bone marrow osteoblasts is a common and critical pathway for cytokine-induced mobilization. *Blood* **114**, 1331–1339 (2009).
48. C. E. Dunbar, K. A. High, J. K. Joung, D. B. Kohn, K. Ozawa, M. Sadelain, Gene therapy comes of age. *Science* **359**, eaan4672 (2018).
49. C. Li, R. J. Samulski, Engineering adeno-associated virus vectors for gene therapy. *Nat. Rev. Genet.* **21**, 255–272 (2020).
50. T. Bozoglu, S. Lee, T. Ziegler, V. Jurisch, S. Maas, A. Baehr, R. Hinkel, A. Hoenig, A. Hariharan, C. I. Kim, S. Decker, H. Sami, T. Koppara, R. Oellinger, O. J. Muller, D. Frank, R. Megens, P. Nelson, C. Weber, A. Schnieke, M. Sperandio, G. Santamaria, R. Rad, A. Moretti, K. L. Laugwitz, O. Soehnlein, M. Ogris, C. Kupatt, Endothelial retargeting of AAV9 in vivo. *Adv. Sci.* **9**, e2103867 (2022).
51. B. Bostick, A. Ghosh, Y. Yue, C. Long, D. Duan, Systemic AAV-9 transduction in mice is influenced by animal age but not by the route of administration. *Gene Ther.* **14**, 1605–1609 (2007).
52. P. Sood, A. Krek, M. Zavolan, G. Macino, N. Rajewsky, Cell-type-specific signatures of microRNAs on target mRNA expression. *Proc. Natl. Acad. Sci. U.S.A.* **103**, 2746–2751 (2006).
53. M. N. McCall, M. S. Kim, M. Adil, A. H. Patil, Y. Lu, C. J. Mitchell, P. Leal-Rojas, J. Xu, M. Kumar, V. L. Dawson, T. M. Dawson, A. S. Baras, A. Z. Rosenberg, D. E. Arking, K. H. Burns, A. Pandey, M. K. Halushka, Toward the human cellular microRNAome. *Genome Res.* **27**, 1769–1781 (2017).
54. L. R. Baden, H. M. El Sahly, B. Essink, K. Kotloff, S. Frey, R. Novak, D. Diemert, S. A. Spector, N. Rouphael, C. B. Creech, J. McGettigan, S. Khetan, N. Segall, J. Solis, A. Brosz, C. Fierro, H. Schwartz, K. Neuzil, L. Corey, P. Gilbert, H. Janes, D. Follmann, M. Marovich, J. Mascola, L. Polakowski, J. Ledgerwood, B. S. Graham, H. Bennett, R. Pajon, C. Knightly, B. Leav, W. Deng, H. Zhou, S. Han, M. Ivarsson, J. Miller, T. Zaks; COVE Study Group, Efficacy and safety of the mRNA-1273 SARS-CoV-2 vaccine. *N. Engl. J. Med.* **384**, 403–416 (2021).
55. F. P. Polack, S. J. Thomas, N. Kitchin, J. Absalon, A. Gurtman, S. Lockhart, J. L. Perez, G. Perez Marc, E. D. Moreira, C. Zerbini, R. Bailey, K. A. Swanson, S. Roychoudhury, K. Koury, P. Li, W. V. Kalina, D. Cooper, R. W. Frenck Jr., L. L. Hammitt, O. Tureci, H. Nell, A. Schaefer, S. Unal, D. B. Tresnan, S. Mather, P. R. Dormitzer, U. Sahin, K. U. Jansen, W. C. Gruber, Safety and efficacy of the BNT162b2 mRNA COVID-19 vaccine. *N. Engl. J. Med.* **383**, 2603–2615 (2020).
56. K. K. Ray, R. S. Wright, D. Kallend, W. Koenig, L. A. Leiter, F. J. Raal, J. A. Bisch, T. Richardson, M. Jaros, P. L. J. Wijngaard, J. J. P. Kastelein, Two phase 3 trials of inclisiran in patients with elevated LDL cholesterol. *N. Engl. J. Med.* **382**, 1507–1519 (2020).
57. H. S. Soifer, T. Koch, J. Lai, B. Hansen, A. Hoeg, H. Oerum, C. A. Stein, Silencing of gene expression by gymnotic delivery of antisense oligonucleotides. *Methods Mol. Biol.* **815**, 333–346 (2012).
58. A. Taleb, P. Willeit, S. Amir, T. Perkmann, M. O. Kozma, M. L. Watzenbock, C. J. Binder, J. L. Witztum, S. Tsimikas, High immunoglobulin-M levels to oxidation-specific epitopes are associated with lower risk of acute myocardial infarction. *J. Lipid Res.* **64**, 100391 (2023).
59. V. J. van den Berg, M. M. Vroegindewey, I. Kardys, E. Boersma, D. Haskard, A. Hartley, R. Khamis, Anti-oxidized LDL antibodies and coronary artery disease: A systematic review. *Antioxidants* **8**, 484 (2019).
60. W. Palinski, S. Horkko, E. Miller, U. P. Steinbrecher, H. C. Powell, L. K. Curtiss, J. L. Witztum, Cloning of monoclonal autoantibodies to epitopes of oxidized lipoproteins from apolipoprotein E-deficient mice. Demonstration of epitopes of oxidized low density lipoprotein in human plasma. *J. Clin. Invest.* **98**, 800–814 (1996).
61. F. Porsch, Z. Mallat, C. J. Binder, Humoral immunity in atherosclerosis and myocardial infarction: From B cells to antibodies. *Cardiovasc. Res.* **117**, 2544–2562 (2021).
62. D. Kitamura, J. Roes, R. Kuhn, K. Rajewsky, A B cell-deficient mouse by targeted disruption of the membrane exon of the immunoglobulin μ chain gene. *Nature* **350**, 423–426 (1991).
63. E. P. C. van der Vorst, S. L. Maas, A. Ortega-Gomez, J. M. M. Hameleers, M. Bianchini, Y. Asare, O. Soehnlein, Y. Doring, C. Weber, R. T. A. Megens, Functional ex-vivo imaging of arterial cellular recruitment and lipid extravasation. *Bio Protoc.* **7**, e2344 (2017).
64. S. E. McGeary, K. S. Lin, C. Y. Shi, T. M. Pham, N. Bisaria, G. M. Kelley, D. P. Bartel, The biochemical basis of microRNA targeting efficacy. *Science* **366**, eaav1741 (2019).
65. R. C. Friedman, K. K. Farh, C. B. Burge, D. P. Bartel, Most mammalian mRNAs are conserved targets of microRNAs. *Genome Res.* **19**, 92–105 (2009).
66. L. Elia, P. Kunderfranco, P. Carullo, M. Vacchiano, F. M. Farina, I. F. Hall, S. Mantero, C. Panico, R. Papait, G. Condorelli, M. Quintavalle, UHRF1 epigenetically orchestrates smooth muscle cell plasticity in arterial disease. *J. Clin. Invest.* **128**, 2473–2486 (2018).
67. K. Nishi, H. Itabe, M. Uno, K. T. Kitazato, H. Horiguchi, K. Shinno, S. Nagahiro, Oxidized LDL in carotid plaques and plasma associates with plaque instability. *Arterioscler. Thromb. Vasc. Biol.* **22**, 1649–1654 (2002).
68. L. Nagy, P. Tontonoz, J. G. Alvarez, H. Chen, R. M. Evans, Oxidized LDL regulates macrophage gene expression through ligand activation of PPARγ. *Cell* **93**, 229–240 (1998).
69. B. H. Li, Y. W. Yin, Y. Liu, Y. Pi, L. Guo, X. J. Cao, C. Y. Gao, L. L. Zhang, J. C. Li, TRPV1 activation impedes foam cell formation by inducing autophagy in oxLDL-treated vascular smooth muscle cells. *Cell Death Dis.* **5**, e1182 (2014).
70. R. Roldan-Montero, J. M. Perez-Saez, I. Cerro-Pardo, J. Oller, D. Martinez-Lopez, E. Nunez, S. M. Maller, C. Gutierrez-Munoz, N. Mendez-Barbero, J. C. Escola-Gil, J. B. Michel, M. Mittelbrunn, J. Vazquez, L. M. Blanco-Colio, G. A. Rabinovich, J. L. Martin-Ventura, Galectin-1 prevents pathological vascular remodeling in atherosclerosis and abdominal aortic aneurysm. *Sci. Adv.* **8**, eabm7322 (2022).
71. S. Andrews. (2010). FastQC: A quality control tool for high throughput sequence data; www.bioinformatics.babraham.ac.uk/projects/fastqc/.
72. M. Martin, Cutadapt removes adapter sequences from high-throughput sequencing reads. *EMBnet.journal* **17**, 10–12 (2011).
73. S. Parekh, C. Ziegenhain, B. Vieth, W. Enard, I. Hellmann, zUMIs—A fast and flexible pipeline to process RNA sequencing data with UMIs. *Gigascience* **7**, giy059 (2018).
74. M. I. Love, W. Huber, S. Anders, Moderated estimation of fold change and dispersion for RNA-seq data with DESeq2. *Genome Biol.* **15**, 550 (2014).
75. X. A. Cambronne, R. Shen, P. L. Auer, R. H. Goodman, Capturing microRNA targets using an RNA-induced silencing complex (RISC)-trap approach. *Proc. Natl. Acad. Sci. U.S.A.* **109**, 20473–20478 (2012).
76. I. Çimen, B. Kocatürk, S. Koyuncu, O. Tufanli, U. I. Onat, A. D. Yildirim, O. Apaydin, S. Demirsoy, Z. G. Aykut, U. T. Nguyen, S. M. Watkins, G. S. Hotamisligil, E. Erbay, Prevention of atherosclerosis by bioactive palmitoleate through suppression of organelle stress and inflammasome activation. *Sci. Transl. Med.* **8**, 358ra126 (2016).
77. I. Cimen, Z. Yildirim, A. E. Dogan, A. D. Yildirim, O. Tufanli, U. I. Onat, U. Nguyen, S. M. Watkins, C. Weber, E. Erbay, Double bond configuration of palmitoleate is critical for atheroprotection. *Mol. Metab.* **28**, 58–72 (2019).
78. T. A. Seimon, Y. Wang, S. Han, T. Senokuchi, D. M. Schrijvers, G. Kuriakose, A. R. Tall, I. A. Tabas, Macrophage deficiency of p38alpha MAPK promotes apoptosis and plaque necrosis in advanced atherosclerotic lesions in mice. *J. Clin. Invest.* **119**, 886–898 (2009).
79. E. Falk, M. Nakano, J. F. Bentzon, A. V. Finn, R. Virmani, Update on acute coronary syndromes: The pathologists' view. *Eur. Heart J.* **34**, 719–728 (2013).

Acknowledgments: We thank E. Erbay (Altos Labs, Bay Area Institute) for the critical reading of the manuscript and M. Haberbosch, C. Bonfiglio, and T. Pitsch for technical assistance. We are grateful to C. Ries and S. Steffens for sharing laboratory equipment. C.W. is a Van de Laar professor of atherosclerosis. **Funding:** This work was supported by the European Research Council (ERC AdG°692511 to C.W.), the Deutsche Forschungsgemeinschaft (DFG, project IDs: 403584255-TRR 267-A2, 390857198-EXC 2145, and SFB1123-A1/A10 to C.W.; SFB1123-B4 to A.S. and M.N.-J.; SFB1123-B5 to D.S.; SFB1123-Z1 to R.T.A.M.; and SFB1123-Z2 to W.E.), the German Centre for Cardiovascular Research (DZHK, project 81Z0600203 to C.W. and D.S.), and a grant from the Interdisciplinary Center for Clinical Research at the RWTH Aachen University (to E.P.C.v.d.V.). **Author contributions:** I.C. designed and performed in vitro and in vivo experiments, immunostaining, and histology; analyzed the data; and drafted the manuscript. L.N., Z.A.K., and E.M.-F. performed functional experiments in vitro and analyzed the data. J.M.H., Y.J., and R.T.A. M. performed and analyzed ex vivo arterial perfusion and in vivo monocyte recruitment assays. F.M.F. performed functional experiments in vitro, generated lentiviral vectors, and analyzed the data. M.A. and S.G. assisted with in vivo experiments for atherogenesis and performed and analyzed flow cytometry. M.N.-J. performed ex vivo live EC imaging experiments. E.B. and W.E. performed and analyzed Prime-seq experiments. J.D., E.P.C.v.d.V., Y.D., and A.S. provided intellectual input and critical reagents. D.S. designed the experiments, interpreted the data, and wrote the manuscript. C.W. conceived and supervised the study, designed the experiments, provided funding, and wrote the manuscript. **Competing interests:** The authors declare that they have no competing interests. **Data and materials availability:** All data associated with this study are present in the paper or the Supplementary Materials.

Submitted 14 October 2022
Accepted 13 October 2023
Published 1 November 2023
10.1126/scitranslmed.adf3357